

RATE OF AIR ESCAPE FROM ROLLS WOUND AT
HIGH SPEEDS WITH A FORCE LOADED NIP

By

HUMAIR AHMED MOHAMMED

Bachelor of Science

Osmania University

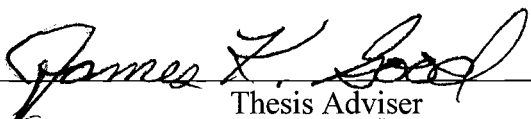
Hyderabad, India

1992

Submitted to the Faculty of the
Graduate School of the
Oklahoma State University
in partial fulfillment of
the requirements for
the Degree of
MASTER OF SCIENCE
May, 1995

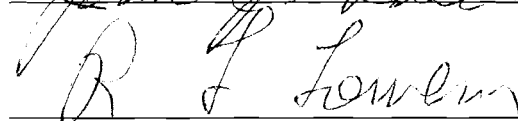
RATE OF AIR ESCAPE FROM ROLLS WOUND AT
HIGH SPEEDS WITH A FORCE LOADED NIP

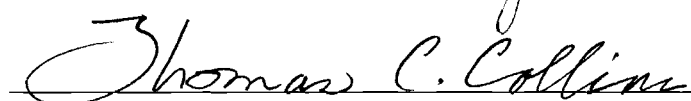
Thesis Approved:



Thesis Adviser







Dean of the Graduate College

ACKNOWLEDGMENTS

I wish to express my sincere appreciation to my advisor, Dr. James K. Good, for his intelligent supervision, constructive guidance, and invaluable assistance . His guidance and active participation throughout this project have been a tremendous asset. I would like to thank him for providing me with this research opportunity and a generous financial support.

I would also like to thank Dr. Richard L. Lowery and Dr. John J. Shelton for serving on my graduate committee. Special thanks are due to Robert Taylor and Ron Markum at the web handling research center, for providing suggestions and assistance during the study.

Most importantly, I would like to express my deepest gratitude and appreciation to my mother, Mrs. Naima Azmath who has supported me morally and financially to this day, and to my late father Mohammed Manzoor Ahmed.

Finally, I would like to thank my loving wife Safia, for her consistent patience and understanding, and providing me with the moral support needed to complete this endeavor.

TABLE OF CONTENTS

Chapter	Page
I. INTRODUCTION	1
II. LITERATURE REVIEW	4
Hakiel's Model	6
Reduced Radial Modulus	9
Squeeze Film Damper Theory	12
III. AIR FILM THICKNESS MODELS	14
Hydrodynamic Equation	14
Elasto-Hydrodynamic Equation	17
Chang's Prediction Equation	19
IV. EXPERIMENTAL SETUP	23
V. MEASUREMENT OF ENTRAINED AIR	27
VI. EXPERIMENTAL RESULTS-SELECTION OF A MODEL FOR AIR FILM THICKNESS	30
Bertram and Eshel's Hydrodynamic Solution	31
Hamrock and Dowson's Elasto-hydrodynamic Solution	32
Chang's Elasto-hydrodynamic Solution	33
Experimental Results	37
Comparison of Theory and Experiment	38
Experimental Observations Using a Metal Nip	41
Effect of Wound Roll Modulus (E_b) and the Modulus of the Nip (E_a) on the Film Thicknes.....	43
VII. RADIAL PRESSURE PROFILE	47
VIII. AIR ESCAPE OVER TIME	51
Comparison of Theory and Experiment	58

Chapter	Page
IX. SUMMARY AND CONCLUSIONS	61
Future Work	62
REFERENCES	64
APPENDIX	65

LIST OF TABLES

Table	Page
I. Volume of Air Collected for Twenty Four Individual Winding Experiments	66
II. Comparison of Theoretical Values from Bertram and Eshel's Hydrodynamic Equation with Experimental Results	67
III. Comparison of Theoretical Values from Hamrock and Dowson's Elasto-hydrodynamic Minimum Air Film Equation with Experimental Results	69
IV. Comparison of Theoretical Values Calculated from Chang's Elasto-hydrodynamic Equation for Compressed Air Film with the Experimental Results	71
V. Comparison of Theoretical Values Calculated from Chang's Hydrodynamic Equation for Decompressed Air Film with the Experimental Results.....	73
VI. Comparison of Theoretical Values Calculated from Chang's Elasto-hydrodynamic Equation for Decompressed Air Film with the Experimental Results	75
VII. Comparison of Experimental Results Obtained from The Rubber Nip and The Hollow Aluminum Nip	77
VIII. Radial Pressures as a Function of Normalized Radius	78
IX. Volume of Air Collected Immediately After Winding as a Function The Length of The Roll Unwound	79
X. Comparison of The Air Collected From Two Rolls Unwound 3 Days After and Immediately After Winding Respectively as a Function of Their Lengths	80
XI. Air Layer Thickness as a Function of Time for Three Sets of Roll Samples	81

XII. Comparison of Theoretical Values Calculated from Squeeze Film Damper Equation With Experimental Results	82
XIII. Comparison of the Range of Dimensionless Parameters Used by Hamrock & Dowson with Those Associated with the Experiments.....	84
XIV. Comparison of The Range of Dimensionless Parameters Used By Chang with Those Associated with the Experiment	85
XV. Individual Effect of Wound Roll Modulus E_b and Nip Modulus E_a on Air Layer Thickness (h_0) Derived by Hamrock and Dowson and by Chang for their Elasto-hydrodynamic Equation's	86

LIST OF FIGURES

Figures	Page
1. Schematic View of the Bubblerimeter	5
2. Air Layer Between Two Web Surfaces Before and After Winding	10
3. Illustration of a Squeeze Film Damper	12
4. Illustration of Nip Roller Assisted Centerwinding	15
5. Variation of R_{eq} as a Function of R_r , the Wound Roll Radius	22
6. Winder Configuration	24
7. Theoretical Results of Bertram & Eshel's Hydrodynamic Equation	32
8. Theoretical Results of Hamrock & Dowson's Elasto-hydrodynamic Equation	33
9. Theoretical Results of Chang's Equation	35
10. Air Film Thickness (h_c) Away From the Nip as Predicted by Chang	36
11. Chang's h_c Prediction Using Bertram and Eshel's Hydrodynamic Term	37
12. Experimental Results	38
13. Air Film Thickness (h_0) for Hamrock and Dowson's and Chang's Equations, as Affected by Wound Roll/Nip Modulus	44
14. Radial Modulus, E_r Computed as a Function of Pressure, P	48
15. Comparison of Radial Pressure as a Function of Normalized Radius (R/R_c)	49
16. Pressure Profile for The Roll with Entrained Air	50
17. Volume of Air Collected at Various Lengths of the Unwinding Roll	53

Figures	Page
18. Comparison of the Volume of Air Collected Immediately and 3 Days After Winding, as the Roll Unwinds	55
19. Air Escape as a Function of Time(Experimental Results)	57
20. Air Escape as a Function of Time(Comparison of Theory and Experiment) .	57
21. Bumps at The Roll Edges Obstructing The Escape of Entrained Air	59
22. Non-Uniform Pressure Distribution Along The Web Width	60

NOMENCLATURE

A	Area of Entrained Air per Unit Width (in. ²)
a	Semi-axis in Transverse Direction of Line Contact (in.)
b	Semi-axis in Motion Direction of Line Contact (in.)
C_1, C_2, C_3	Polynomial Coefficients
E_a	Modulus of the Nip (675 psi.)
E_b	Modulus of the Wound Roll (psi.)
E_c	Modulus of the core (30×10^6 psi.)
E_r	Radial Modulus of the Wound Roll (psi.)
E_t	Tangential Modulus of the Wound Roll (psi.)
$E_{r \text{ air}}, E_r \text{ air}$	Modulus of the Web with the Entrained Air (psi.)
$E_{r \text{ stack}}, E_r \text{ stack}$	Modulus of the Web as a Stack of Layers (psi.)
$E_{r \text{ eq}}, E_r \text{ eq}$	Combined Stack and Air Radial Modulus (psi.)
E, E'	Effective Modulus (psi.)
F	Normal Applied Load (including the tension component)
f_r, f_b	RMS of ball, race (RMS of the web substituted for both) (in.)
G	Dimensionless Materials Parameter
g^2	Ratio of Tangential Modulus to Radial Modulus of the Wound Roll
H	Air Layer Thickness
h	Thickness of the Web (in.)
h_c	Air Film Thickness After Expansion (in.)
h_0	Minimum Air Film Thickness (in.)
h_1, h_2	Air Layer Thickness (in.)
K_{air}	Stiffness of Air Layer Entrained (lbf/in.)
K_{stack}	Stiffness of a Stack of Web Layers (lbf/in.)

K_{eq}	Combined Stiffness of Stack and Air Layer (lbf/in.)
k	Ellipticity Parameter ($k = 10$ for line contact)
L	Load per Unit Width to Overcome Air Entrainment effects(lbf/in.)
P_a	Atmospheric or Ambient Pressure (psi.)
P_0	Pressure Beneath the outer Layer (psi.)
R_x, R_e	Effective Radius (1.085 in.)
R_n, R_g	Radius of the Nip (2.0 in.)
R_o, R_r	Radius of the Wound Roll (2.3715 in.)
t	Time (secs.)
T	Web line Tension (0.48 lbf/in.)
T_w	Winding Tension (1000 psi.)
U	Dimensionless Speed Parameter
u	Winding Speed (in./sec.)
u	Average of Nip and Roll Velocities (in./sec.)
u_a	Velocity of the Nip (in./sec.)
u_b	Velocity of the Wound Roll (in./sec.)
W	Dimensionless Load Parameter
x	Radial Compression of Entrained Air Layer During Winding (in.)
ϵ_r	Radial Strain (in./in.)
ϵ_t	Tangential Strain (in./in.)
Λ	Dimensionless Film Parameter
μ	Dynamic Viscosity of Air (2.6×10^{-9} lbf-sec./in. ²)
ν	Poisson's Ratio
ν_a	Poisson's Ratio of the Nip (0.4)
ν_b	Poisson's Ratio of Roll (0.01)
ν_{rt}	Poisson's Ratio in the Radial Direction
ν_{tr}	Poisson's Ratio in the Tangential Direction
σ_r	Stress in the Radial Direction (psi.)
σ_t	Stress in the Tangential Direction (psi.)

CHAPTER I

INTRODUCTION

Thin plastic films which are widely used for a variety of industrial applications such as packaging, magnetic recording etc. are usually wound in spirals to form a roll . In general any film that can be wound into a roll is called a web. The film may be paper, cloth or plastic. Perhaps the most widely used films today are plastic films used for a variety of applications ranging from packaging to magnetic recording media. The most commonly used polymers are polyethylene, polypropylene, cellulose acetate and polyethylene terephthalate.

These films are wound by a variety of winding techniques, the most common being centerwinding. In centerwinding we have a core that is subjected to a torque. A motor provides torque to the core and controls the speed of winding. In centerwinding, we may have a lay-on roller whose function is mainly to squeeze the unwanted excess air entrained between two adjacent layers as the roll builds up. At low winding speeds an increase in the wound-in-tension has been documented without being forced to increase the web line tension. This lay-on roller is sometimes called a nip roller. Alternately we have surface winding in which the torque is provided to a lay-on roller, which applies a

normal force to the core and drives it as a result of contact friction, at a speed at which it is driven by the motor.

Trapping too much air between layers is highly undesirable because it prevents the inter-layer contact, resulting in slippage in the axial direction, more commonly referred to as “telescoping”. Air entrainment radically decreases the stress state within a wound roll thereby adversely affecting the integrity of the roll structure during storage and shipment. Air entrainment can be reduced by increasing the web line tension during winding but this is much less effective than the use of a nip. In addition, winding a roll too tightly may result in defects such as wrinkling and starring, thereby degrading the quality of the roll. Thus it is important for the wound roll to have an optimum stress level, neither too low (e.g. as a result of air entrainment) so as to cause telescoping, nor too high so as to degrade the roll quality.

A variety of factors need to be considered to assess the state of stress in wound rolls. The most relevant factors are web tension, radius of wound roll, presence of entrained air as well as the material properties of the web in consideration. A factor that affects the amount of entrained air and could thereby appreciably affect the stress state in wound rolls is the velocity at which the roll is wound (i.e. the “winding velocity”).

Winding velocity is to be considered to take into account the amount of air that is carried along the web during winding, to be trapped subsequently in the adjacent layers. Rolls wound at higher velocities are prone to entrain more air than those at lower velocities.

To increase the efficiency of a winding operation it is necessary to incorporate higher winding velocities and to reduce the effect of air entrainment. A nip roller serves

mostly to accomplish the above by allowing us to keep the winding velocity high while keeping the entrained air thickness low. This study seeks to investigate the air entrainment rates during high speed winding, and how these would affect the physical properties of the wound roll. Furthermore it will examine the rate at which the entrained air discharges from the wound roll over a period of time.

CHAPTER II

LITERATURE REVIEW

Air entrainment experiments in centerwound rolls with a lay on roll (nip roller) were done and analyzed by Covell [5] in his thesis "*The effect of a nip roller on entrained air during high speed winding*". Covell performed experiments in which he collected the residual air which had been entrained at various web velocities and nip loads. He compared his results to a Hydrodynamic relationship which was derived by Bertram and Eshel [1] and an Elasto-Hydrodynamic relationship derived by Hamrock and Dowson [9]. Covell's experimental data correlated best with the Hydrodynamic Equation.

Previously, related work on air entrainment was done by Bouquerel [3]. In his thesis "*Theoretical and experimental study of winding of thin plastic films: Aerodynamic effects*", Bouquerel attempted to experimentally verify Hamrock and Dowson's [9] elasto-hydrodynamic equation. But due to inadequate correlation between the theoretical and experimental values he had to introduce a correction factor. He calculated the apparent density of the roll based on its mass and external diameter and finally deduced the air layer thickness assuming incompressible film of known density and that the density of air is negligible as opposed to the web material (Polyester in his experiment).

To measure the entrained air accurately a direct measuring technique was employed by Covell [5]. A bubble collection apparatus, also called as the “Bubblimeter” (See Fig. 1), was developed. It consists of a rectangular water tank fixed with a spool and a 45° dead bar. The wound roll is placed on the spool and the web is directed out of the water tank to the winding machine by means of the 45° dead bar. The wound roll placed in the apparatus is subsequently unwound at a low speed, thereby ensuring all the air bubbles are trapped in the conical hood placed directly over the roll on side supports fixed inside the tank. The amount of air that is collected inside the hood is quantified by collecting it into a graduated cylinder fixed to the top of the hood.

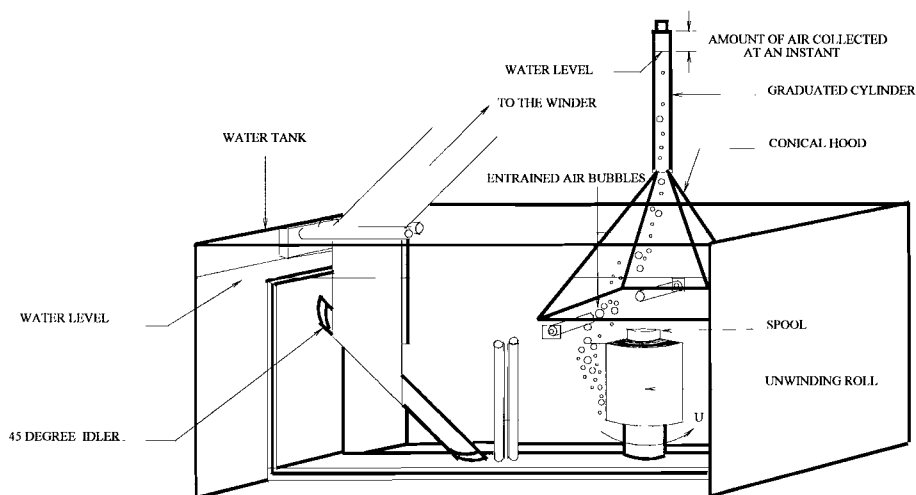


Figure 1. Schematic View of the Bubblimeter.

Covell conducted his experiments on 48 gage Type 442 Polyester, 6 inches wide and 1500 m long, at a winding tension of 1000 psi, and at various velocities and nip

loads. The experimental results obtained were compared with theoretical values from Hamrock and Dowson's [9] Elasto-hydrodynamic equation as well as Bertram and Eshel's [1] Hydrodynamic equation. Using a multiplicative correction factor a modified version of the Elasto-hydrodynamic equation seemed to give a close approximation for the air layer thickness over the tested range of winding conditions. However, when compared without any modification his experimental values were closest to the theoretical results derived from Bertram and Eshel's [1] Hydrodynamic equation.

Before discussing the algorithms that can be used to model the entrained air it is necessary to first understand the basic winding models that deal with the stress distribution in wound rolls and second how these stresses are affected by the presence of entrained air. One such classical model was presented by Hakiel [8] which has since been modified by Good, Wu and Fikes [7] to include a nip roller. The Hakiel model as well as the stresses in the wound rolls due to the presence of entrained air are presented briefly in the following pages.

Hakiel's Model

Hakiel [8] in 1987 presented a winding model which applied a finite difference method to solve a second order non-linear differential equation in radial pressure. Young's modulus in the radial direction was made a function of radial pressure. The non-linear orthotropic hoop model developed by Hakiel assumes:

1.) The wound roll to be a cylinder made by winding concentric hoops of web, and that the properties of the roll as each hoop is added are constant.

2.) The roll has a linear elastic behavior in the tangential direction and a non linear elastic behaviour in the radial direction which varies as a function of radial stress.

3.) Plane stresses which are functions of the radial positions only and axial stresses are zero.

Hakiel begins with the equilibrium, constitutive and compatibility equations respectively in cylindrical coordinates:

$$r \left(\frac{d\sigma_r}{dr} \right) + \sigma_r - \sigma_t = 0 \text{ ----- Equilibrium Eq.} \quad (1)$$

The linear orthotropic constitutive equations for radial and tangential directions are

$$\epsilon_r = \left(\frac{1}{E_r} \right) \sigma_r - \left(\frac{\nu_{rt}}{E_t} \right) \sigma_t$$

and (2A & 2B)

$$\epsilon_t = \left(\frac{1}{E_t} \right) \sigma_t - \left(\frac{\nu_{tr}}{E_r} \right) \sigma_r \text{ respectively.}$$

Using the strain energy constraint, $\nu_{tr} E_t = \nu_{rt} E_r$ and defining , $g^2 = \frac{E_t}{E_r}$, we have

$$\epsilon_r = \left(\frac{1}{E_t} \right) (g^2 \sigma_r - \nu \sigma_t)$$

and ----- Constitutive Eqs. (2A' & 2B')

$$\epsilon_t = \left(\frac{1}{E_t} \right) (\sigma_t - \nu \sigma_r) \text{ respectively.}$$

Finally from the linear definitions of strain in cylindrical coordinates we have

$$r \left(\frac{d\epsilon_t}{dr} \right) + \epsilon_t - \epsilon_r = 0 \text{ ----- Compatibility Eq.} \quad (3)$$

Combining Eqs. (1) (2) & (3) yields a second-order differential equation in terms of radial pressure as

$$r^2 \left(\frac{d^2 \sigma_r}{dr^2} \right) + 3r \left(\frac{d\sigma_r}{dr} \right) - (g^2 - 1) \sigma_r = 0 \quad (4)$$

This equation is solved several times during the execution of the model such that $g(r)$ and the boundary conditions can be updated. Thus the model is solved for increments in pressure, which are summed to $\delta(P(r))$ as shown in Eq.(5). As the roll builds up so does the pressure, assuming δP as the incremental change in pressure at radius r , Eq.(4) can be modified as

$$r^2 \left(\frac{d^2 \delta P}{dr^2} \right) + 3r \left(\frac{d\delta P}{dr} \right) - (g^2 - 1) \delta P = 0 \quad (5)$$

The above is a second order differential equation with non-constant coefficients and is subject to two boundary conditions, the first of which is obtained by equating the radial deformation of the first layer with the deformation of the core. In terms of the variation of pressure, δP , due to the addition of the last layer this boundary condition becomes:

$$\left. \frac{\partial \delta P}{\partial r} \right|_{r=1} = \left(\frac{E_t}{E_c} - 1 + \nu \right) \delta P \Big|_{r=1} \quad (6)$$

and the second is given by the hoop stress formula as

$$\delta P \Big|_{r=s} = \frac{T_w h}{r} \quad (7)$$

After each solution of Eq.(5) the new increment in pressure $\delta P(r)$ must be summed with all previous increments to yield $P(r)$ or

$$P_i = \sum_{j=1}^n \delta P_{ij} \quad (8)$$

where P_i is the pressure in a certain radial sector and Eq.(5) would be solved n times.

Solving the above boundary value problem numerically, Hakiel [8] modeled the radial stress distribution inside the wound roll. This model has been modified by Good, Wu and Fikes [7] in “*The Internal Stresses in Wound Rolls with the Presence of a Nip Roller*”.

Reduced Radial Modulus

A reduction in radial modulus is one way in which air entrainment may be incorporated into Hakiel’s model. To determine the radial modulus as a function of the air layer thickness, a radial modulus of air between the layers must be determined. Good and Holmberg [6] in “*The Effect of Air Entrainment in Centerwound rolls*”, describe a relationship for the radial modulus which is reduced by the entrained air. Assuming that the trapped air is an ideal gas under isothermal conditions, we can apply Boyle’s law as follows

$$h_0(p_0 + p_a) = h_1(p + p_0 + p_a) \quad (9)$$

where, h_0 and h_1 are the initial and final air layer thickness, P_0 and P_a are the initial pressure between the layers and atmospheric pressure respectively, and P is the pressure applied to compress the layer from h_0 to h_1 , as depicted in the illustration below:

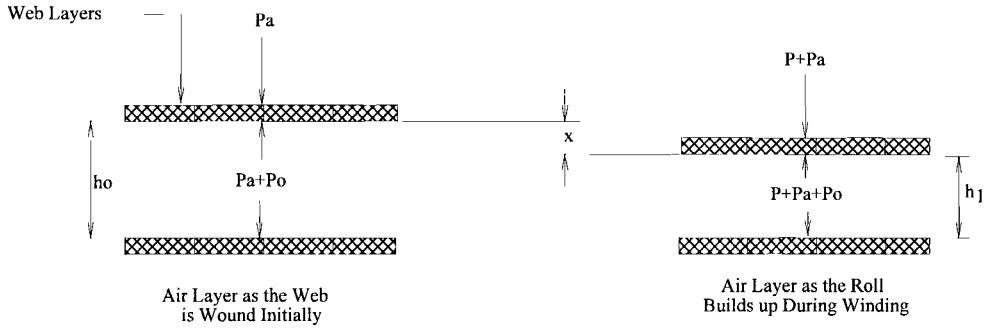


Figure 2. Air Layer Between Two Web Surfaces Before and After Winding.

From Fig. 2,

$$h_1 = h_0 - x \quad (10)$$

Eq. (9) can thus be written as

$$h_0(P_0 + P_a) = (h_0 - x)(\sigma_r + P_0 + P_a) \quad (11)$$

Solving for x and dividing both sides by h_0 we get a pseudo expression for the radial strain of the trapped air layer as

$$\frac{x}{h_0} = \frac{\sigma_r}{(\sigma_r + P_0 + P_a)} = \epsilon_r \quad (12)$$

Inverting Eq. (12) after taking its derivative with respect to the radial pressure yields

$$E_{r \text{ air}} = \frac{(\sigma_r + P_0 + P_a)^2}{(P_0 + P_a)} \quad (13)$$

The modulus of the entrained air and that of the stack of web layers can be modeled as springs in series whose equivalent stiffness can be written as

$$\frac{1}{K_{eq}} = \frac{1}{K_{stack}} + \frac{1}{K_{air}} \quad (14)$$

In terms of E_r the above equation becomes

$$\frac{1}{\left(\frac{E_{req} A}{h_0 + h}\right)} = \frac{1}{\left(\frac{E_{r stack} A}{h}\right)} + \frac{1}{\left(\frac{E_{r air} A}{h_0}\right)} \quad (15)$$

Simplification yields

$$E_{req} = \frac{(h_0 + h)}{\left(\frac{h}{E_{r stack}}\right) + \frac{h(P_0 + P_a)}{(\sigma_r + P_0 + P_a)^2}} \quad (16)$$

$E_{r stack}$ is a material property and can be obtained from a material testing system. It is imperative to mention here that the difference between air layer thickness and the surface roughness of the film determine which one of the above expressions is applicable. For the winding conditions three possibilities may exist,

1) If the air layer is less than the mean surface roughness of the film the air layer is not a factor since the asperities contact the web surface and hence E_r need not be modified.

2) If air layer is less than the maximum asperity height but greater than the mean surface roughness of the web then a combination of $E_{r air}$ and $E_{r stack}$ i.e., E_{req} (Eq. (16)) should be used.

3) If air layer thickness is greater than the maximum asperity height then the expression for $E_{r air}$ (Eq. (13)) should be used.

Squeeze Film Damper Theory

The following section is devoted to a latter part in this study which deals with the escape of entrained air over time from wound rolls. The theory developed herein would be used to model the rate of air escape.

Blevins [2] in *Applied Fluid Dynamics Handbook* describes a squeeze film damper as shown below

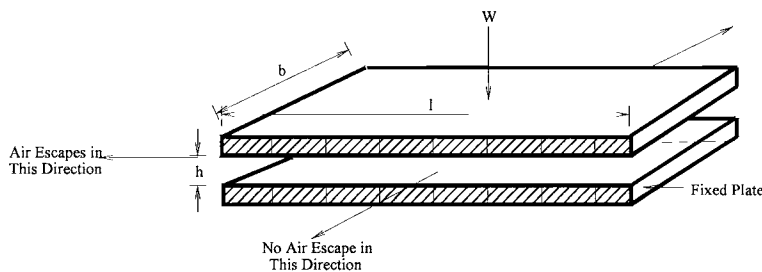


Figure 3. Illustration of a Squeeze Film Damper.

The bottom plate is assumed to be fixed and the upper one is allowed to fall down freely under its own weight W , and that the air present between the two plates squeezes out only along the width, L . No air escapes along the length, b . Assuming that the upper plate is falling down from a height h_1 to h_2 then an expression for the time needed to close the gap from h_1 to h_2 can be written as:

$$t = \frac{\mu b L^3}{2W} \left[\frac{1}{h_2^2} - \frac{1}{h_1^2} \right] \quad (17)$$

where,

μ is the dynamic viscosity of air, $2.7 \cdot 10^{-9}$ lbf - sec / in.²

L is the dimension parallel to which air escapes, in.

b is the dimension perpendicular to which air escapes, in.

W is the weight of the plate, lbf.

t is time in seconds required for the air layer to decrease from h_1 to h_2 .

The above equation can be used to predict air escape over various time periods, assuming the two plates to be a pair of overlapping web layers present in a wound roll.

The roll width can be substituted in place of L and the ratio W/bL can be simply substituted knowing the value of the radial pressure P, since $P = W/bL$.

CHAPTER III

AIR FILM THICKNESS MODELS

Hydrodynamic Equation

Bertram and Eshel [1] in "*Recording Media Archival Attributes*" published a formula in 1980 which relates the nip load to air layer thickness and winding velocity, viscosity, tension and geometry. Their experimental procedure involved an indirect method of measuring air layer thickness, wherein pull tabs were used to measure interlayer pressures and quantifying interlayer slippage during rapid deceleration to give an estimate of entrained air (The back emf generated by the decelerating roll was related to the inertia of the roll which changes with the amount of air entrapped). However their experiments do not check the validity of their formula. The present study starts off by verifying the accuracy and applicability of the Hydrodynamic Equation to the actual winding conditions using centerwinding with a nip roller.

The Hydrodynamic Equation has been derived using the pressure distribution on the nip (See Fig. 4) which is governed by Reynolds equation:

$$\frac{dp}{dx} = \frac{12\mu u}{h_0^2} \left(\frac{1 - \frac{h^*}{h_0} + \frac{x^2}{2R_e h_0}}{\left[1 + \frac{x^2}{2R_e h_0} \right]^3} \right) \quad (18)$$

with boundary conditions,

$$p = p_a + \frac{T}{R_0} \quad \text{at } x = 0 \quad (19)$$

$$p = p_a \quad \text{at } x = \infty \quad (20)$$

where h^* is the thickness of the air gap at which $dp/dx = 0$.

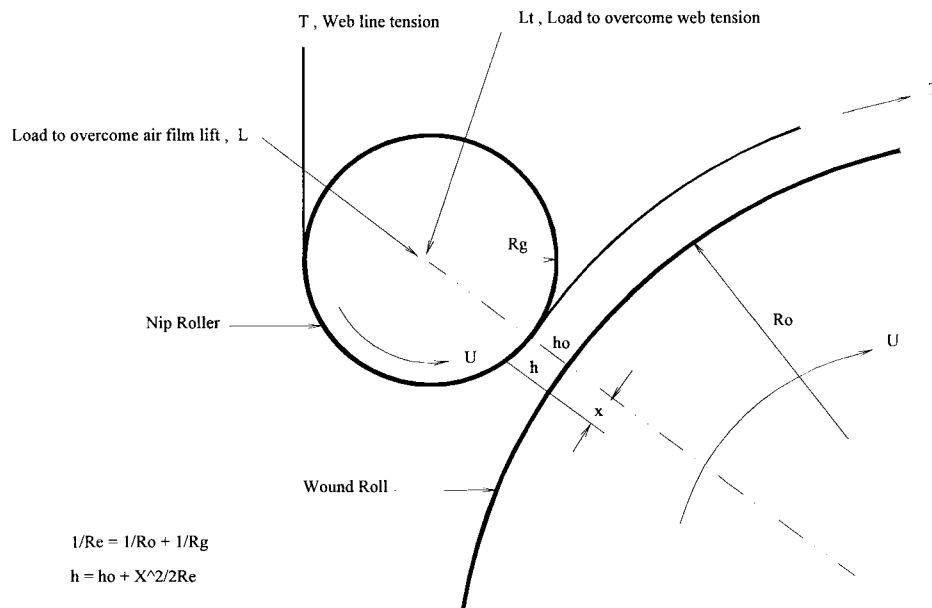


Figure 4. Illustration of Nip Roller Assisted Centerwinding.

Integrating for pressure distribution and subsequent simplification yields the nip load required to overcome the air entrainment effects as:

$$L = \int_0^{\infty} p dx \quad (21)$$

$$L = \frac{4\mu UR_e}{h_0} + \frac{4T\sqrt{2R_e h_0}}{3\pi R_0} \quad (22)$$

This equation does not solve for h_0 explicitly instead it solves for the load required to overcome air entrainment effects. Thus to find h_0 at a given value of L we should initially have a spreadsheet program that gives us the value of L for various values of h_0 . It should be noted that the second term of Eq.(22) is minute when compared to the first term, thus,

$$h_0 \approx \frac{4\mu UR_e}{L} \quad (23)$$

Assuming the expansion of entrained air at ambient temperature after it passes away from under the nip the thickness of the air film (h_c), due to a change in the velocity profile, becomes $4h_0/3$ as reported by Chang [4]. Thus Eq. (23) can be modified to include compressibility effects as follows:

$$h_c \approx \frac{4h_0}{3} = \frac{4}{3} \left(\frac{4\mu UR_e}{L} \right) \quad (24)$$

Hence,
$$h_c \approx \frac{16}{3} \frac{\mu UR_e}{L} \quad (25)$$

Elasto-hydrodynamic Equation

Hamrock and Dowson [9] in “*Ball Bearing Lubrication*” present a formula to calculate the film thickness between two bodies in elliptical contact. However, this equation can also be extended for use with two bodies in line (rectangular) contact as referenced in their study. Their elliptical contact theory is composed of 11 critical parameters. From these parameters they established 5 dimensionless groupings which can be related to the film thickness as follows:

$$H = f(k, U, W, G) \quad (26)$$

where, k represents an ellipse of deformed contact with a major axis of dimension $2a$ and a minor axis of dimension $2b$. For line contact,

$$k = \frac{a}{b} \cong 10 \quad (27)$$

U is the dimensionless speed parameter which can be defined as

$$U = \frac{\mu u}{E' R_x} \quad \text{where} \quad u = \frac{u_a + u_b}{2} \quad (28)$$

W represents the dimensionless load parameter and can be written as

$$W = \frac{F}{E' R_x^2} \quad \text{where} \quad R_x = \frac{1}{\frac{1}{R_n} + \frac{1}{R_r}} \quad (29)$$

and G is a dimensionless material parameter which is represented as

$$G = \frac{E'}{1/\alpha} \quad \text{where} \quad E' = \frac{2}{\frac{1-v_a^2}{E_a} + \frac{1-v_b^2}{E_b}} \quad (30)$$

α is the pressure-viscosity coefficient of lubrication (m^2/N).

Note that for W to be dimensionless F must have units of load (lbf or N) in Eq.(29)

After the dimensionless parameters were grouped, each was varied keeping the rest constant to observe each parameter's influence on the film thickness, and the proportionality equations obtained were subsequently formulated each depicting its influence on the film thickness.

$$\frac{h_0}{R_x} \propto (1 - 0.85e^{-0.31k}) \quad (31)$$

For $k = 10$, we have

$$\frac{h_0}{R_x} \propto 0.962 \quad \Rightarrow \frac{h_0}{R_x} \approx 1 \quad (32)$$

$$\frac{h_0}{R_x} \propto U^{0.65} \quad (33)$$

$$\frac{h_0}{R_x} \propto W^{-0.21} \quad (34)$$

It is important to note here that G , the material property parameter did not affect h_0/R_x for the range of low elastic modulus materials in Hamrock and Dowson's study.

Hence G is missing in the film thickness equation which is now presented.

Hamrock and Dowson set reasonable ranges of the dimensionless parameters W and U for various types of oil and grease lubricated bearings. They then solved coupled sets of Reynold's and Elasticity equation's to yield the film thickness, h_0 . From the results obtained a least-squares curve fit was used to develop a formula, for film thickness h_0 as a function of the dimensionless parameters, called as the Elast-Hydrodynamic Equation which is:

$$h_0 = R_x 7.43(1 - 0.85e^{-0.31k})U^{0.65}W^{-0.21} \quad (35)$$

and for our case where $k = 10$, the above equation reduces to:

$$h_0 = R_x 7.43U^{0.65}W^{-0.21} \quad (36)$$

Since the Elasto-hydrodynamic Equation is derived using a curve fit, its applicability may be governed by the range of values for U and W used during the curve fit process. The range of values for U and W used by Hamrock and Dowson for deriving the film thickness equation (Eq. (35)) have been presented in Table XIII in the Appendix. Before proceeding with a comparison of the theoretical models it would be appropriate to introduce a few shortcomings of the Elasto-hydrodynamic equation,

- 1) This equation was derived from a curve-fit technique that was performed on a finite domain of dimensionless parameters.
- 2) The application of this equation to two cylinders in rolling contact is not clear even though it has been referenced in its study.

Chang's Prediction Equations

Chang [4] reported an air film thickness formula developed using a procedure similar to the one used to develop the Elasto-hydrodynamic Equation of Hamrock and Dowson, however it takes into consideration the compressibility effects of air. According to this theory the air film while passing under the force-loaded nip roller gets compressed but expands subsequently as it passes away from it. Chang has presented a set of analytical models for soft and hard materials with negligible and significant

compressibility effects. The present study falls into the category of soft materials since the nip used is made of rubber and since there is air entapped within the wound roll.

Chang has grouped three dimensionless parameters viz., speed, load and material properties respectively as under:

$$H = f(U, W, G) \quad (37)$$

where,

$$U = \frac{\mu u}{P_a R_x} \quad (38)$$

$$W = \frac{F}{P_a R_x} \quad (39)$$

$$G = \frac{E}{P_a} \quad \text{where} \quad E = \frac{1}{\frac{1 - \nu_a^2}{E_a} + \frac{1 - \nu_b^2}{E_b}} \quad (40)$$

Note that for W to be dimensionless F must have units of load per unit width (pli or N/m) in Eq.(39)

A procedure similar to that of Hamrock and Dowson's was employed by Chang to predict the individual dependencies of the dimensionless parameters (The range of values for U , W and G used by Chang for deriving the film thickness equation have been presented in Table XIV in the Appendix) on the air film thickness h_0 . Finally a curve fit was done which in his case showed a perfect correlation with the numerical values.

Based on this he defined the air film thickness h_0 as follows:

$$h_0 = R_x 8.5U^{0.72}W^{-0.5}G^{-0.48} \quad (41)$$

In his study Chang has also developed a relationship for an air film thickness, h_c which is the expanded thickness of the air film after it passes away from under the nip where it

gets compressed. The dependencies of the U, W and G parameters for this case have been formulated as under:

$$h_c = R_x 12.5U^{0.71}W^{-0.2}G^{-0.23} \quad (42)$$

Eq.'s (41) & (42) are to be used for cases where the effective modulus (equivalent modulus of nip and wound roll) ranges from 700 psi. to 5000 psi. For cases where the effective modulus ranges between 100 psi. and 700 psi. the above equations have been modified by Chang as follows:

$$h_0 = R_x 4.8U^{0.66}W^{-0.35}G^{-0.47} \quad (43)$$

$$h_c = R_x 7.4U^{0.66}W^{-0.21}G^{-0.33} \quad (44)$$

The three theoretical air entrainment algorithms described above will be used as a basis for comparing the results obtained experimentally. The one that can closely predict the air film thickness will be used to model the experimental values. Although the value of the air layer thickness as implied from the equations above appears to be a constant, actually it is a function of the radius of the winding roll which keeps increasing till the end of the winding operation. A change in the wound roll radius R_r will change the value of R_{eq} in the calculations for the air film thickness thereby affecting the value of h_0 . In an attempt to assess the variation of R_{eq} , various values of R_{eq} were determined at various wound roll radii and the results plotted as shown in the figure below:

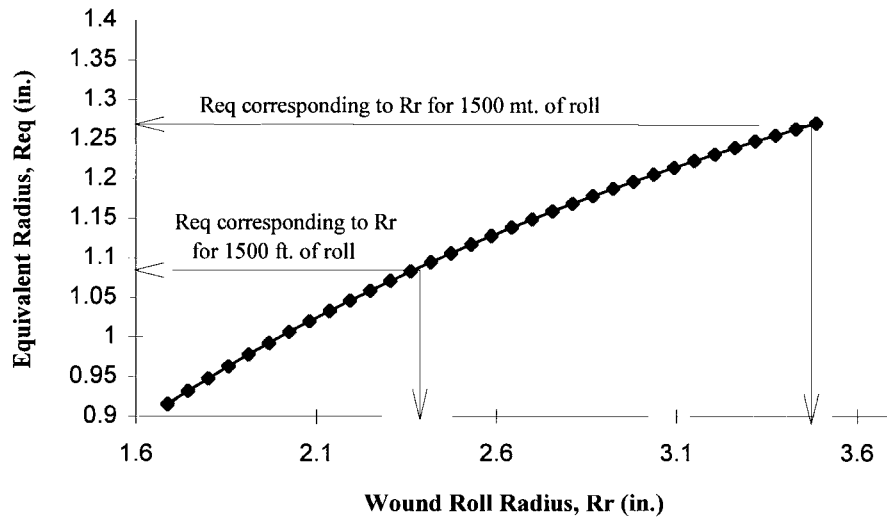


Figure 5. Variation of R_{eq} as a Function of R_r , the Wound Roll Radius.

For the present study the length of the web selected for winding was 1500 ft, referring to Fig. 5 it can be observed that for this length of the roll there is a very little change in the value of R_{eq} . R_{eq} starts off at .92 inch and rises to only 1.09 inches for 1500 ft of roll wound. Even for a 1500 m (4921 ft) long web (selected by Covell[5]) the value of R_{eq} rises to only 1.27 inches. Thus, the simplifying assumption of an *average* air layer thickness will be a sufficient approximation for the air layer thickness, throughout the roll. After selecting an algorithm for the air layer thickness, h_0 , it will be used to develop an equation for a reduced radial modulus which in turn may be used to predict the radial pressure profile using Hakiel's [8] winding model.

CHAPTER IV

EXPERIMENTAL SETUP

Precise measurement of entrained air is a crucial factor in air entrainment studies and in the subsequent winding model development. Measurement of entrained air has posed a subtle problem in the past. Researchers have relied on indirect techniques for measuring entrained air e.g., by using pull tabs for measuring inter-layer pressures and deducing air layer thickness thereon and relating air layer thickness to inter-layer slippage during rapid deceleration[1], or by using the apparent density of the wound roll to estimate the air layer thickness[3]. In contrast Good and Holmberg [6] in "*The Effect of Air Entrainment in Centerwound Rolls*", have employed a sophisticated technique for measuring air layer thickness directly using laser reflectance probes. Using an expression for air layer thickness derived by Knox and Sweeney [11] they were successful in correlating the theoretical and experimental results. However, this technique was limited to the cases where the entrained air layer thickness was greater than .0001inch which is quite small for air films wound in to centerwound rolls but large for air air films wound into centerwound rolls *with a nip*.

In this study "Air Collection" has been accomplished by a direct technique which can be used irrespective of the surface roughness of the web material. The idea is simply

to unwind a wound roll under water, trap all the air bubbles that are released and quantify them to give a measure of the entrained air. The apparatus used to accomplish this is the “Bubblimeter” which has been described briefly in Chapter II (See Fig. 1).

Another factor that needs close observation during centerwinding with a nip roller is the nip load, because, even small nip loads can significantly reduce the amount of air entrained. It is important that the nip should be able to deliver a constant force throughout the winding operation to get a good estimate of the air layer thickness during air entrainment studies with a nip roller. This is especially important when the nip loads used are small because phenomenon such as nip roll bounce etc., get amplified leading to a bad estimate of the air layer thickness. Thus, we have to ensure that the nip roll and the wound roll remain in contact, and the nip load is held constant throughout winding.

It was for the above mentioned facts that before proceeding with the air entrainment studies a new nip was designed on the existing winder, a schematic of which is shown below:

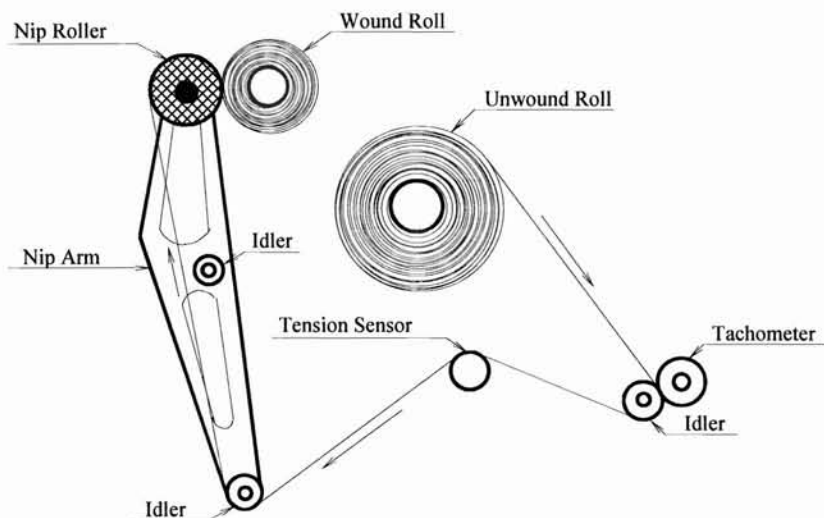


Figure 6. Winder Configuration.

The new nip was designed to operate pneumatically. It was held in position exactly parallel to the wound roll by means of two arms extending on either sides, of which, one extreme (top one) held the nip, and the other (bottom one) an idler. This idler was used to direct the web from the tension sensor to the nip, the web after embracing the nip passes on to the wound roll. Since the nip arms were long and flexible in bending another idler was added in the center as a reinforcement, which later on served to redirect the web from the “Bubblimeter” to the winder. With the existing setup it is possible to perform surface winding by adding a belt, that would drive the nip instead of the wound roll shaft.

After the nip was designed it was configured with the existing winder. The next step was to install a mechanism that would deliver a constant force to the nip arms, which in turn would be delivered to the wound roll during winding. The response of the nip to the applied load had to be sensitive, especially when the loads applied were small. In other words, the mechanism that operates the nip should have the least reaction forces, which otherwise would oppose the nip force and subsequently diminish it.

There were two possibilities, one was to use a dead weight to apply the nip load and the other was to use a piston-cylinder arrangement that would drive the nip pneumatically. The former option was ruled out in lieu of the high winding speeds needed for the experimentation, and the fact that nip roll bounce would make the dead weights almost weightless. This setup was used by Covell[5] and he reports of nip roll bounce problems associated with it. So, the use of a piston-cylinder arrangement was studied. One disadvantage however, was the traction force inside the cylinder due to the

presence of friction. This had to be minimized in order for the nip to deliver small loads consistently.

After examining the working of a variety of piston-cylinder arrangements a specially designed mechanism that works with a minimal traction force was selected. This is manufactured by Origa Corp. has a stroke of eight inches and delivers a maximum force of 65 lbf at a pressure of up to 100 psi which is controlled using an air pressure regulator. The frequency response of air regulators can easily be less than 1 Hz. A wound roll with but one abnormality in its surface can provide a 150 Hz input to the nip roll. Hence, in order to improve its performance a 2 cu.ft. air tank was used to store and deliver the regulated air pressure to the cylinder. The advantage of such a configuration is, we have a large volume of compressible air whose pressure is not easily affected due to nip roll bounce during high speed winding. This is much superior to connecting the air cylinder directly to an air regulator, due to the poor frequency response of air regulators and to a relatively small volume of air (e.g., typically only that in the air supply tubing) which can be compressed. Thus, with this design the nip load will be as constant as possible throughout the winding operation. The minimum force that can be delivered is 2 lbs and 0.5 lb (0.083 pli for a 6 inch wide roll) increments have accurately been resolved using a force gage.

With the nip design complete, a 5 hp AC vector drive was added to drive the winder to speeds in excess of 2000 feet per minute which were controlled by a digital controller with an accuracy of ± 10 feet per minute.

CHAPTER V

MEASUREMENT OF ENTRAINED AIR

This study comprises of two parts, the first one attempts to verify a winding model that incorporates the entrained air immediately after winding. The second part deals with the discharge of entrained air over a period of time and attempts to test the applicability of a “*Squeeze Film Damping Equation*” [See Eq. (17), Chapter II] to estimate the rate of air escape from the wound roll. Thereafter a suitable relationship can be developed or the existing one modified to correlate the experimental results with the theoretical values predicted by the “*Squeeze Film Damping Equation*”.

For performing air entrainment tests Type 442 Polyester Gage 48, 6 in. wide, 1500 ft. long was used. It has a mean surface roughness of 0.27μ in., an RMS surface roughness of 0.42μ in., and a maximum asperity height of 0.78μ in.. The tangential modulus of the web is 600,000 psi.. The web was wound on a 3.375 inches O.D. steel core with an I.D. of 3 inches. A typical O.D. for a 1500 ft roll was 4.7 inches and for the 1500 m rolls which were wound the O.D. was 7 inches.

The reason for using polyester was the need for a non-permeable web material that would not allow the air to diffuse in the radial direction, so that the air that would escape could only do so through the edges of the roll out into the atmosphere. Further,

the thickness of the entrained air layer should be greater than the mean surface roughness of the film, otherwise the air layer would not be a factor at all in the experiments (See Chapter II, Reduced Radial Modulus). For this reason the film chosen for this study has a very low surface roughness in order to ensure that the air collected would produce an average thickness of more than the surface roughness of the web.

The experimental procedure involves winding 1500 ft. of web at various web line velocities and various nip loads at a constant winding tension of 1000 psi. and unwinding the roll in the bubblerimeter. The entrained air collected in ml. is then converted into an average air layer thickness throughout the roll by the following relation:

$$h_0 = \frac{0.06102(\text{Vol. of air in ml.})}{1500*12*6} \quad (45)$$

It has to be noted here that h_0 the air layer thickness is an *average* air layer thickness and not the absolute thickness of the air entrained between each layer. The latter is dependent upon the radius of the wound roll and is not constant for each pair of overlapping layers. Thus the simplifying assumption of an average value makes other calculations less complex and avoids the present study from wandering off into an entirely different aspect of air entrainment which might need the measurement of the volume of air extracted as a function of radius of the wound roll.

All materials have a finite surface roughness. Even if we use a material with very small roughness values it is unlikely that a pair of contacting layers would do so perfectly. There would always be some amount of air trapped in between their asperities.

This air however, would be present under any circumstances irrespective of winding conditions. Even with very large nip loads and low web velocities, conditions that are favorable for flushing out maximum air from between the two contacting faces, there always will be some trapped air called as the “*baseline*” amount of air. This baseline air should not be included in the same category as the entrained air, hence, from all the experimental air collected the baseline amount will be deducted to avoid bias. In an experiment to measure the baseline air 1500 ft. of roll was wound at a speed of 20 fpm and a 32 lbf nip load (conditions favorable to flush out maximum air) and was subsequently unwound in the bubblerimeter. It was found that the baseline amount was about 10 ml, an average for two roll samples. Further an additional correction factor of 3% has been introduced to account for the slight vacuum present in the graduated cylinder of the bubblerimeter. This factor would also be subtracted from all experimental data along with the baseline amount. Table I in the Appendix displays the air collected from 24 individual winding experiments.

CHAPTER VI

EXPERIMENTAL RESULTS - SELECTION OF A MODEL FOR AIR FILM THICKNESS

Experiments were performed at four different winding speeds, ranging from 500 fpm to 2000 fpm, and air was collected for six different values of nip loads corresponding to each speed. Since the intent of this study is to show how the air layer thickness would be affected even with small nip loads, a major portion of the discussion would be done for small nip loads. However the data obtained at higher nip loads would also be presented and discussed briefly.

The results of the experiments were coded into a spreadsheet program and three dimensional surface plots were obtained. These plots show how the air layer thickness varies as a function of web speed and nip load. Theoretical results were obtained by substituting the material properties, winding conditions and other relevant parameters into the Hydrodynamic and Elasto-Hydrodynamic Equations respectively. The parameters used to model these equations can be found in the Nomenclature. The theoretical results were also plotted against the corresponding speeds and nip loads used for experimentation, and a comparison was made. Tables II, III, IV, V & VI in the Appendix

Appendix display the data calculated from the theoretical models and compare it with the experimental results.

Bertram and Eshel's Hydrodynamic Solution

The Hydrodynamic Equation predicts an exponentially decreasing air layer thickness as we proceed towards increasing nip loads and an almost linear decay towards low winding speeds (See Fig. 7). Referring to Eq. (22) (See Chapter III) the only parameters than need to be varied are the nip load L (psi) and the winding velocity U (inches/sec). The values of the constant parameters viz., μ , R_e , R_o and T can be found in the Nomenclature section. The values of L were varied from 4 to 48 lbf (experimental values) and those of U from 500 to 2000 fpm (experimental values) and h_0 was subsequently determined for 24 different combinations of L and U . Maximum air entrainment as expected is observed for the highest speed and the lowest nip load i.e., 2000 fpm and 4 lbf. respectively and the lowest entrainment for high nip loads and low winding speed i.e., 500 fpm and 48 lbf. respectively. The range of average air layer thickness as depicted in the theoretical results was of the order of 6.7μ inch, corresponding to a high of 6.9μ inch, and a low of 0.2μ inch.

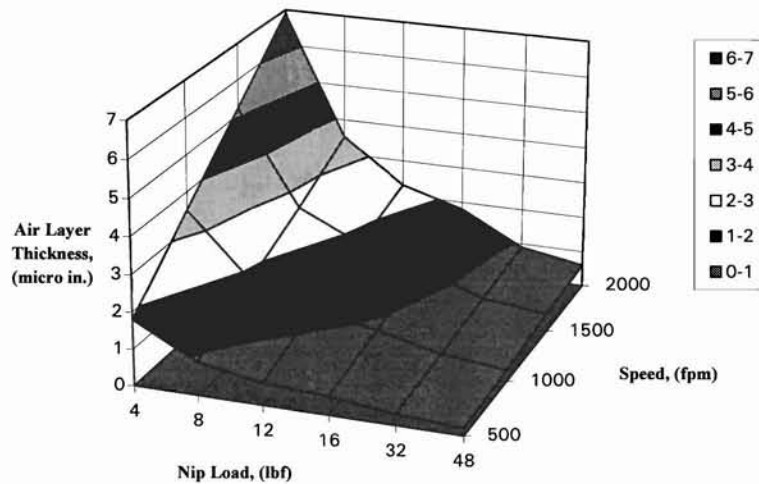


Figure 7. Theoretical Results of Bertram & Eshel's Hydrodynamic Equation.

Hamrock and Dowson's Elasto-hydrodynamic Solution

The Elasto-hydrodynamic Equation predicts a higher range of average air layer thickness, of the order of 20.4μ inch, corresponding to a high of 27.3μ inch and a low of 6.9μ inch. Referring to Eq. (36) (See Chapter III) the values of speed, u (inches/sec) and the normal applied nip load, F (lbf) were similarly varied as in the previous case. The elasto-hydrodynamic equation also uses the effective modulus, E' (modulus of the wound roll and the nip roll), hence the same was determined for different values of the radial modulus, E_r of the wound roll under different nip loadings, and incorporated into Eq (36). The constant parameters used viz., k , μ and R_x have been declared in the Nomenclature. Again the values of L were varied from 4 to 48 lbf and those of u from 500 to 2000 fpm

and h_0 was determined for 24 different combinations of L and u . A distinctive feature of the Elasto-hydrodynamic equation is a far less drastic decrease in air film thickness towards higher nip loads and a much thicker air layer. It should be noted that the dimensionless parameters used by Hamrock and Dowson do not fall in the same range as the dimensionless parameters associated with these experiments (See Table XIII in Appendix).

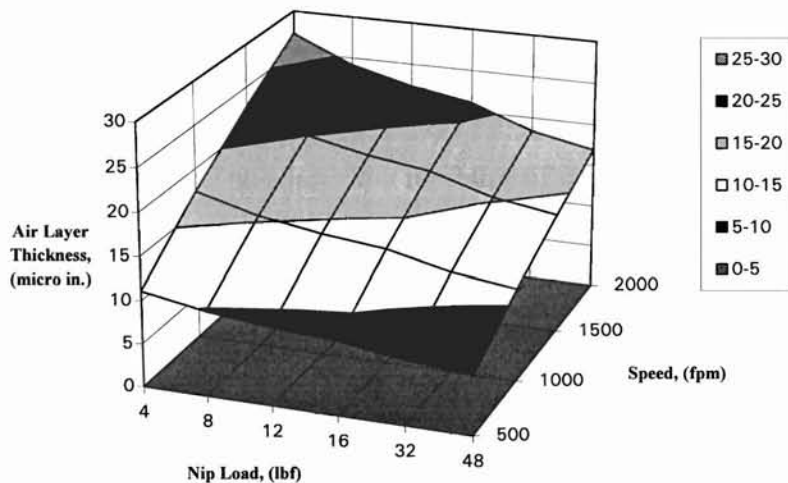


Figure 8. Theoretical Results of Hamrock & Dowson's Elasto-hydrodynamic Equation.

Chang's Elasto-hydrodynamic Solution

Another theoretical model that was recently developed by Chang [4], which takes into account the compressibility effects of the entrained air has also been presented here.

Recall that Hamrock and Dowson's Elasto-hydrodynamic equation is meant for oil film lubrication in ball bearings whereas in air entrainment studies we are dealing with an air film. Chang's model takes into consideration the above disparity where, for air, its density is dominated by pressure unlike the density of oil which is almost unaffected by a wide range of pressures. This model assumes two rotating rollers without a web in between them and that the materials in consideration are isotropic. Here the formula for air layer thickness was again derived using a similar, but not identical set of non-dimensional parameters used by Hamrock & Dowson. This equation too is derived using a curve fit, however the dimensionless parameters associated with these experiments fall in the same range as the ones used by Chang to derive the film thickness relationship (See Table XIV in the Appendix). The equivalent modulus of the nip roll and the wound roll as calculated by the effective modulus E' expression was 750 psi. on an average hence Eq.'s (41) and (42) would be used for the present study. The parameters used to determine the air film thickness (h_0) using Eq. (41) (See Chapter III) are shown in Table XIV, again the values of speed, u (inches/sec) and the nip load per unit width of the roller, F (pli) were varied in a similar way as described previously and the results plotted for their 24 different combinations

Chang's model predicts a thicker air layer than that predicted by the Elasto-hydrodynamic Equation but the rate of decrease of air layer as we proceed towards higher nip loads seems to relate more with the Hydrodynamic Equation than with the Elasto-hydrodynamic equation.

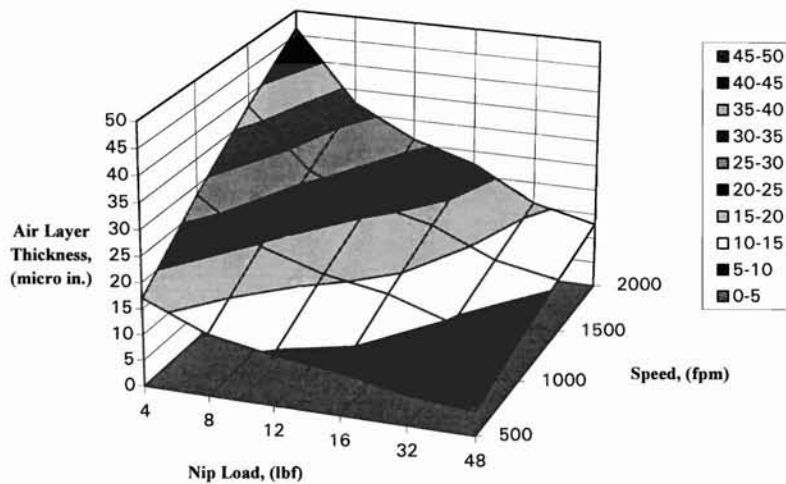


Figure 9. Theoretical Results of Chang's Equation.

All the results plotted above display the *minimum* air film thickness (h_0), the thickness of the air film under the nip. Chang has also developed a relationship for the air film thickness (h_c), the thickness of the air film after it passes away from the nip (See Chapter III, Eq.(42)). This is a more practical case where the air film after getting compressed under the nip expands when it moves away from it. The results obtained due to these compressibility effects are presented in Fig.10. Note that this expression for h_c (Eq. (42)) depends upon a elasto-hydrodynamic term. As is obvious the air film thickness (h_c) predicted after it expands is way too high than the experimental values however the interesting feature to note here is its similarity with the trend observed for Hamrock and Dowson's Elasto-hydrodynamic equation results (unlike the trend observed for h_0 , which resembled Bertram and Eshel's Hydrodynamic equation).

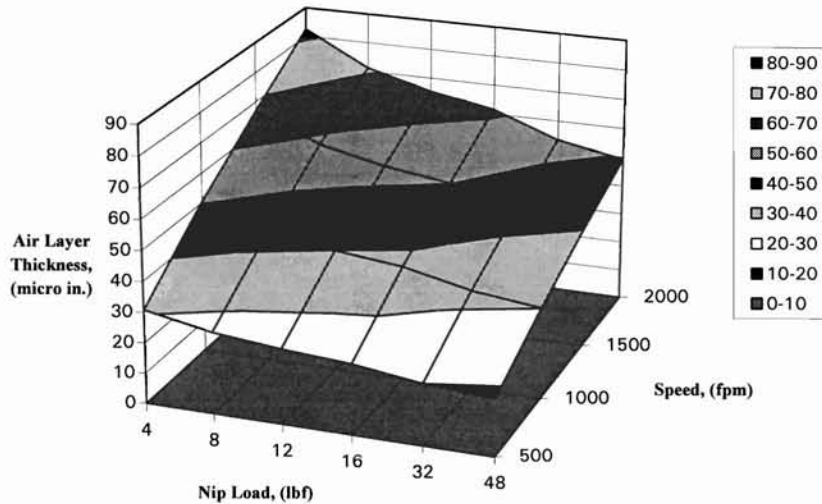


Figure 10. Air Film Thickness (h_c) Away From the Nip as Predicted by Chang.

The results of the h_c relationship developed by Chang utilizing the Elasto-hydrodynamic term is shown above. Chang had also developed another h_c relationship using a hydrodynamic term from Bertram and Eshel's Hydrodynamic equation by suitably modifying it to include the compressibility effect of the air film as it passes away from the nip (See Eq (25), Chapter III). The results of Chang's modification of h_0 to include the compressibility, using the hydrodynamic term are presented in Fig. 11. As is obvious referring to Eq.(25), the results obtained here are simply the results for h_0 predicted by the hydrodynamic equation *times* the factor 4/3 used to modify Eq. (23) to include the change in velocity profile as a result of the compressibility effects of the air film as it passes away from under the nip.

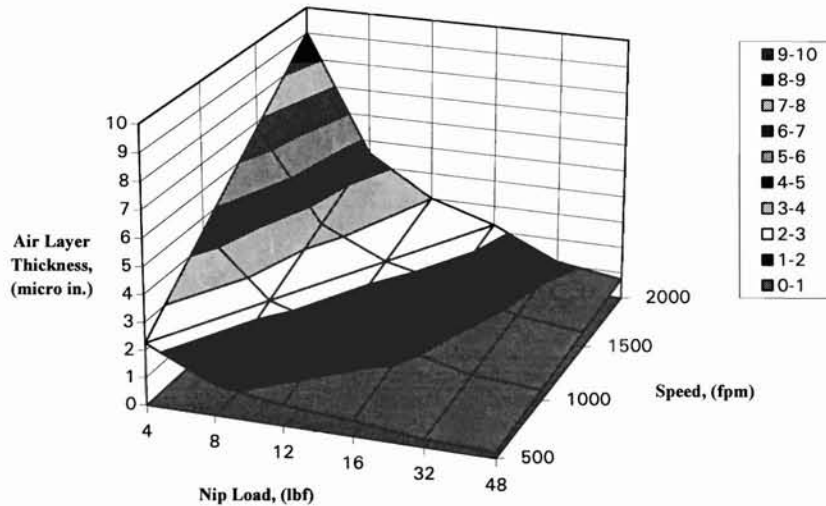


Figure 11. Chang's h_c Prediction Using Bertram and Eshel's Hydrodynamic Term.

Experimental Results

Finally, the experimental results obtained for 24 different tests are presented below with the air layer thickness plotted as a function of nip load and web velocity. There are some random values in the data taken at high speeds that do not compare with the expected results, this may be attributed to the instability of the nip roll and the nip roll bounce associated with those speeds. Repeated tests at high speeds would have produced reasonable values but the amount of material available for the same was limited. Above all, on an average, the experimental results produced consistent values which seemed to follow Chang's h_0 predicted values closely. The trend however resembles more like his h_c model and also the Elasto-hydrodynamic model.

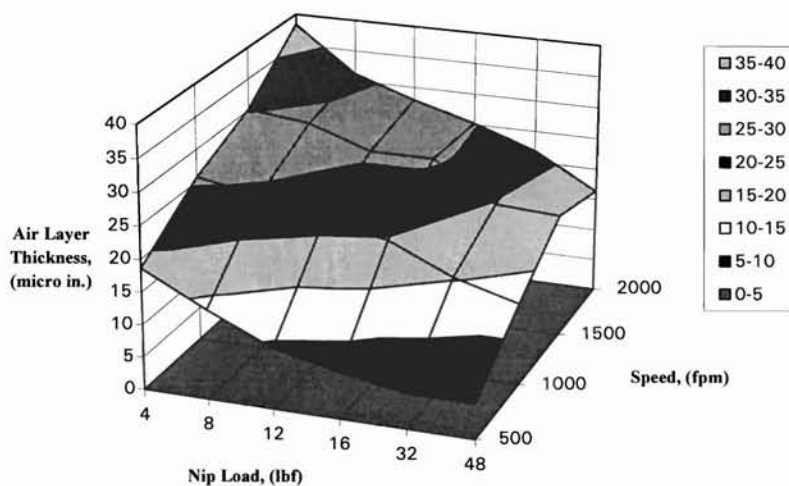


Figure 12. Experimental Results.

Comparison of Theory and Experiment

Comparing the values of the air layer obtained experimentally with the theoretical values it can be observed that Chang's model for the minimum film thickness (h_0) is the closest to the experimental results. However when we observe the 3-dimensional surface plots the trend appears to resemble Chang's model for the expanded air film thickness (h_c). Also note the similarity with the Elasto-hydrodynamic equation results. Some of the other notable features are, at small values of nip loads the experimental results closely follow Chang's h_0 prediction (e.g., at 4lbf nip load), even the rate of decrease of h_0 appears to be similar. Towards very high values of nip loads the experimental results are

more closer to Hamrock and Dowson's Elasto-hydrodynamic equation results (e.g., at 48lbf nip load). This suggests a more predominant elasto-hydrodynamic regime at high nip loads.

An interesting feature in the Elasto-hydrodynamic lubrication studies is the film parameter, Λ , which is related to the lubrication film thickness (air film thickness in our case) as follows:

$$\Lambda = \frac{h_0}{\sqrt{(f_r^2 + f_b^2)}} \quad (46)$$

where f_r and f_b both are rms surface roughness of the film and h_0 is the film thickness.

The film parameter, Λ is used to identify the lubrication regime. Hydrodynamic or fluid-film lubrication occurs when the contacting surfaces are separated by a lubricating film so thick, they cease to contact. It has been reported by Hamrock and Dowson [9] that in this regime the value of Λ is greater than 10 and may be as high as 100. Elasto-hydrodynamic lubrication occurs when the bearing materials are soft such as elastomers and rubbers, where the local elastic deformation of the bearing surfaces allows for a coherent lubricating film and surface contact is not fully avoided as in the previous case. The film parameter in this regime falls between 3 and 10. For the existing winding conditions we calculated the values of Λ , which were found to range from 9 to 65. This implies that we have a predominant hydrodynamic regime for most of the winding conditions with a borderline between hydrodynamic and elasto-hydrodynamic regimes. The above phenomenon as predicted by the film parameter Λ contradicts the experimental results which have predicted a predominant elasto-hydrodynamic regime. The validity of using

the film parameter, Λ (which is simply a ratio of film thickness to the surface roughness), to judge the regime of lubrication is questionable. The film parameter Λ was calculated in the context of ball bearing lubrication (where the supporting materials are rigid and do not experience significant deformation), whereas in the present case we are dealing with a rubber nip roll and an air entrained wound roll with the air beneath the nip, during winding, exerting a couple of 100 psi. pressure sufficient enough to deform the surfaces in contact and produce a predominant elasto-hydrodynamic regime (encountered with soft bearing materials) rather than a hydrodynamic regime (encountered with rigid rollers).

Tables II, III, IV, V & VI in Appendix compare the results presented in the figures above. a)The Hydrodynamic equation predicts an air layer roughly six times less than the experimental results. b)Hamrock and Dowson's elasto-hydrodynamic equation slightly underestimates the experimental values at small values of nip load but at higher nip loads, (e.g., 48 lbf) it yields good results. c)For majority of the experimental results Chang's h_0 prediction values follow reasonably well, except of course for the extreme nip loads. d)Finally, comparing Chang's h_c (derived using Chang's elasto-hydrodynamic term) values we observe that they overestimate the experimental results almost by a factor of 2. Also it may quite be possible that we are underestimating the experimental values instead, as a result of air escape even before we can practically measure it in the procedure employed in the experiments. More insight can be had in this particular phenomenon in the next chapter where we study rate of air escape from wound rolls.

Since Hamrock and Dowson's elasto-hydrodynamic equation and Chang's prediction equation's were formulated based on a curve fit technique using dimensionless

parameters corresponding to a set of input values, it was necessary to have an idea as to how close the dimensionless parameters dictated by the existing winding conditions were to the one's used to derive the above equations.

With the ellipticity parameter, k , held constant, the load, W and speed, U parameters were the only variables that needed to be compared with the range of dimensionless parameters used by Hamrock & Dowson to obtain the curve fit. Table XIII in Appendix shows a comparison between the range of dimensionless parameters used by Hamrock & Dowson to those associated with the experimental conditions. It is quite clear that the dimensionless parameters U and W corresponding to the practical case deviate far from those that were considered by Hamrock and Dowson to derive their elasto-hydrodynamic equation (Eq.(35)).

Table XIV in the Appendix provides a similar comparison for the range of U , W and G values used by Chang to curve fit and derive his film thickness equation. It can be seen that the range of values for the dimensionless parameters dictated by the existing winding conditions fall within the same range of theoretical values used by Chang in his film thickness equation derivation. Thus Chang's model should provide a sound basis of comparison with the experimental results.

Experimental Observations Using a Metal Nip

To verify the authenticity of the experimental data one of the experiments was repeated using a new nip configuration. The new nip was made of Aluminum, unlike the

previous one which was made of rubber thus having different material properties. Two different sets of rolls, one 1500 ft. long and the other 1500 m long were wound at 2000 fpm, 8 lbf nip load and 1000 psi. web tension. Air was collected immediately after the winding operation. Table VII in Appendix displays the results recorded for the same.

It was expected that the experiments would yield different results due to different material properties of the nip, on the contrary the values obtained were almost the same as the ones obtained with the rubber nip, for both lengths of the roll. The reason for this can be attributed to the fact that the experiment using the metal nip which was performed for the 2000 fpm winding velocity and 8 lbf nip load combination corresponds to a predominant hydrodynamic regime where the web layers tend to lose contact during winding, also the equivalent modulus corresponding to this case (in fact for all the nip loads used) confirms to the range where it is not affected much by any further increase in the modulus of the nip roll therefore the amount of air entrapped remains unaffected. (This has been proved in the next section, see page 43). During winding at high speeds (e.g. 2000 fpm) and small nip loads (e.g. 4,8 lbf) a comparatively thicker air film develops and exerts a pressure force on both the wound roll and the nip roll sufficient enough for preventing each from coming in contact with the other at times during winding thereby keeping the film thickness unaffected by the nip and the wound roll moduli.

Effect of Wound Roll Modulus (E_b)
and the Modulus of the Nip (E_a) on the Film Thickness

In order to determine how important the moduli of the nip roll and the wound roll are for affecting the effective modulus and thus the air film thickness, a sensitivity study was performed on both Hamrock and Dowson's and Chang's Elasto-hydrodynamic equations (Eq's (35) &(41) respectively). The value of E_a was held constant and E_b was varied to calculate various values of h_0 and vice versa. The comparisons are made at a reference speed of 2000 fpm and 8 lbf nip load (a combination quite frequently used all through the experimental study). It was observed during the calculations that a change in the radial modulus of the wound roll, E_b above a certain value, ceased to have a noticeable effect on the value of the air film thickness h_0 . Above a certain value for E_b the calculations started yielding a constant value for E' , the effective modulus, hence leading to constant air film thickness. This phenomenon was observed in both Hamrock and Dowson's and Chang's equations. The results of these calculations are tabulated in Table XV in the Appendix and plotted as shown in the figure below:

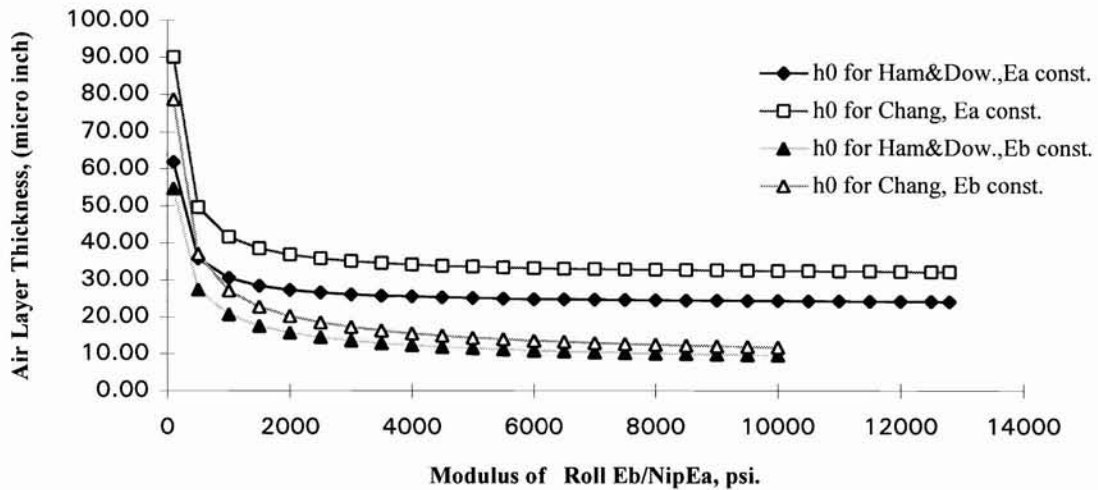


Figure 13. Air Film Thickness (h_0) For Hamrock and Dowson's & Chang's Equations, Eq's (35) & (41) respectively as Affected by Wound Roll/Nip Modulus.

It is quite evident from Fig. (13) that the modulus of the wound roll and the nip roll radically affect the air film thickness, however only for small values (< 1000 psi.) of E_a or E_b . There is a drastic change in the air film thickness (h_0) when the modulus of the wound roll is varied below about 1000 psi.. Above about 1000 psi. hardly any change is noticed. A similar trend is observed with the nip roll modulus, E_a also. However it is the wound roll modulus which is affected by the entrained air hence the focus of this discussion would be the wound roll modulus E_b and the radial modulus of the wound roll E_r .

The values of E_b were obtained by contact tests performed by Covell [5] using Tekscan which is a PC based instrument for pressure or force measurements. It consists of a force sensitive resistor and an expansion card that allows the PC to record and display non-uniform loads measured. The peak pressure under the nip was measured for different nip loads and was substituted in a theoretical expression ,Eq. (47), derived by Xu [12] for $E_{r \text{ contact}}$ in the absence of air

$$E_{r \text{ contact}} = aP + bP^2 + cP^3 \quad (47)$$

where

$$a = 3138.0 \quad b = -33.54 \quad c = 0.151$$

The calculated radial modulus of the winding roll, E_b was then used to model the elasto-hydrodynamic equations.

It has to be noted here that E_b was measured statically, a condition which is very different from the one when the roll is wound at 2000 fpm. Various phenomenon can be encountered in the latter case, one of which that has been mentioned earlier is the possible loss of contact between the nip and the wound roll at high speeds and small nip loadings. In such cases a static determination of E_b is obsolete. It will be shown in the next chapter that air entrainment reduces the modulus of the wound roll radically and that the wound roll modulus is a dynamic quantity, varying as a function of the radius. Hence a radial modulus of the wound roll E_r should be used for the modulus of the wound roll. But E_r and h_0 , the air film thickness, are dependent on each other, this makes the determination of E_r or h_0 more complicated since neither can be isolated from the other. Hence a safer approximation would be to use the static values of E_b obtained through contact tests, for

air film thickness calculations. The range of values for E_b obtained during the contact tests [5] varied from 8200 psi corresponding to a 4 lbf nip load to about 47000 psi for 48 lbf nip load. All of these fall in the range where their variation does not have any noticeable effect on h_0 .

CHAPTER VII

RADIAL PRESSURE PROFILE

To develop a radial pressure profile we need to know the dynamic values of E_r , the radial modulus, which can be formulated simply by a stress-strain relationship. E_r , which is a “pseudo material property” can be measured using the INSTRON, by placing a stack of webs and measuring the strain produced by them due to the application of a compressive force. The value stress/strain would then give the modulus, E_r . However, in the realm of air entrainment studies E_r , cannot be static, since, in the stack tests if an air layer comparable to the one entrained during winding is present then the value of strain would go up, thereby decreasing the value of E_r and vice versa. Thus in practicality we have different air layer thickness at different radii in a wound roll (recollect that the *average* air layer thickness is only a simplifying assumption), these differences contribute to the variations in E_r at various radii of the wound roll. It was for this reason that different E_r values were formulated using a curve fit [10], resulting in a third degree polynomial expression which is:

$$E_r = C_1P + C_2P^2 + C_3P^3 \quad (46)$$

where C_1 , C_2 , and C_3 are constants derived from stack tests.

For $E_{r \text{ stack}}$, the constants are:

$$C_1 = 129.0 \quad C_2 = -0.037 \quad C_3 = 4.0e-4$$

Applying Eq.(16) for $E_{r\text{ eq}}$, yields the following constants:

$$C_1 = 60.0 \quad C_2 = 0.416 \quad C_3 = -0.001$$

Simialarly, for $E_{r\text{ air}}$, application of Eq.(13) yields:

$$C_1 = 3.042 \quad C_2 = 0.0475 \quad C_3 = 1.097e-4$$

These relationships between E_r , the radial modulus and P, the radial pressure can be depicted as follows:

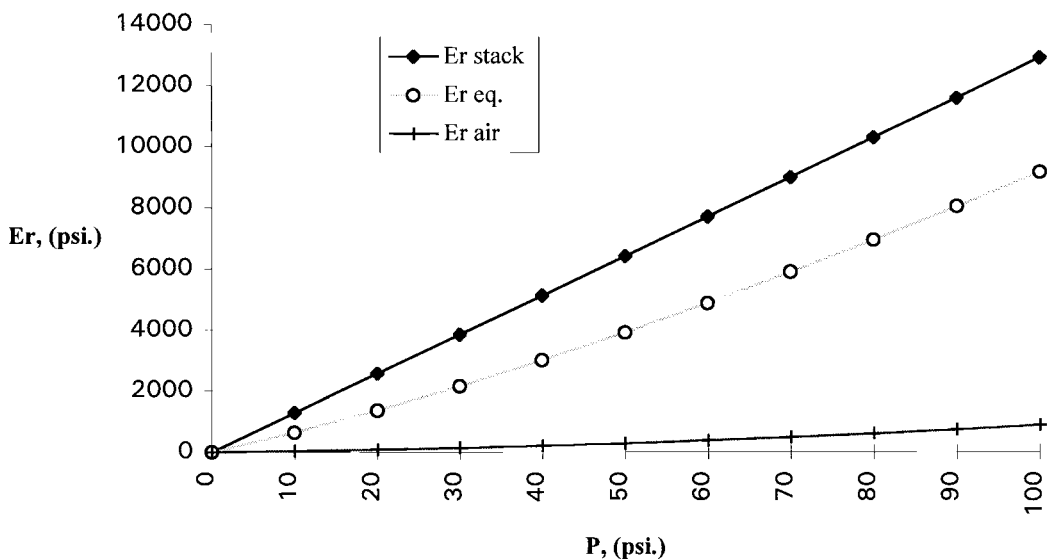


Figure 14. Radial Modulus, E_r Computed as a Function of Pressure, P.

Once the various expressions for E_r are developed we can predict the radial pressure profiles using the software WINDER v 4.0 available at WHRC. This software takes the values of the roll radius, winding speeds, winding tensions, radius of core and

its material properties, dimensions of the web in consideration and its material properties and the constants obtained from the stack tests as input and plots the radial pressure profile. Fig.15 depicts the radial pressure profiles obtained using $E_{r, \text{stack}}$, $E_{r, \text{eq}}$ and $E_{r, \text{air}}$ respectively on a common axes:

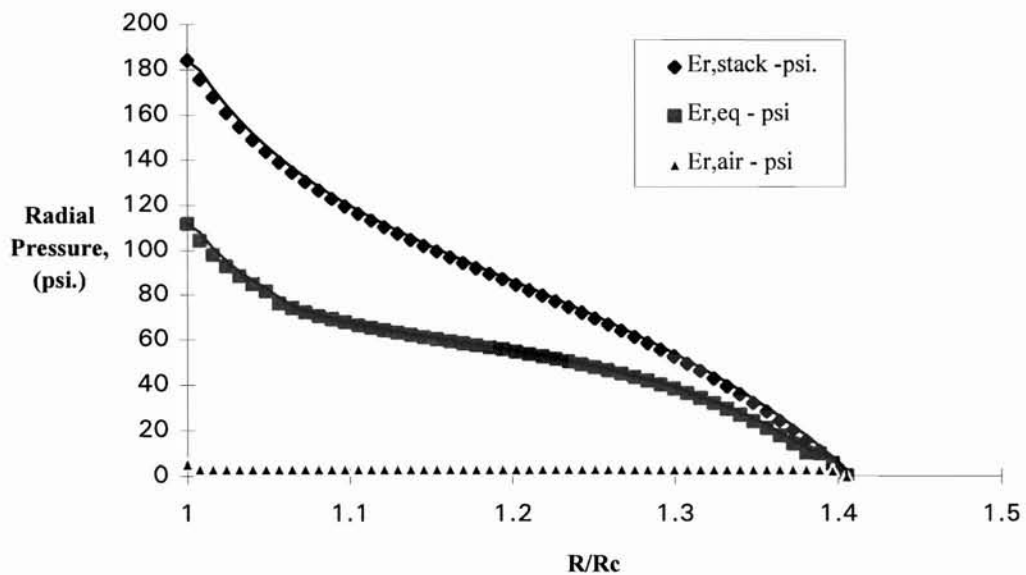


Figure 15. Comparison of Radial Pressure as a Function of Normalized Radius (R/R_c).

As is evident from the above figure the entrained air reduces the radial pressure at the mid-point of the roll to 3 psi. when compared with the stack and equivalent values, which are 85 psi. and 55 psi. respectively. Table VIII in Appendix depicts the range of pressure distribution over the radius of a wound roll. Fig. 16 shown below displays a detailed pressure profile for the roll entrained with air, the object of experimentation,

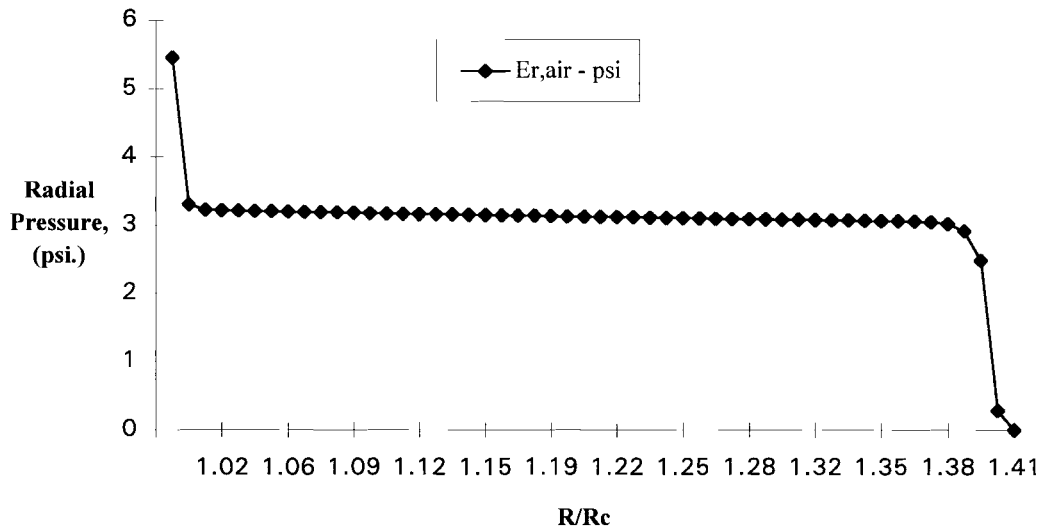


Figure 16. Pressure Profile for the Roll with Entrained Air.

The above plot represents a typical characteristic of the pressure profile when the ratio of E_t/E_r is high. The maximum pressure is present at the core and soon becomes a more or less constant value till it reaches the outer radii of the core, where it sharply decreases to zero for the outermost layer.

CHAPTER VIII

AIR ESCAPE OVER TIME

It has been analytically proven by three different air entrainment models and experimentally proven in this study that as the winding speeds increase the amount of trapped air also escalates. If the amount of air trapped is very large e.g., during high speed centerwinding without a nip roller, it is quite possible that there will not be any inter-layer contact of the web material, and the web layers might ride completely upon the air layers, this phenomenon is referred to as *aeroplaning*. Only at the roll edges, where the air has a good chance of discharging to the atmosphere does the possibility of layer to layer contact exist. This loss of contact between the adjacent web layers would lead to a decreased resistance to the slippage of the web axially, resulting in telescoping and other roll defects. In order to overcome this problem it is important that the underlying mechanism that operates during and after winding and which affects the rate of air entrainment and escape respectively, be studied.

Up to this point in the study the former mechanism was studied, and now the study will concentrate on the phenomenon of air escape from rolls and how it affects the integrity of the roll. In order to evaluate the rate at which the air escapes a set of rolls were wound under similar nip loads and at constant web velocities and were unwound at

various lengths in time. The set of rolls 1500 ft. long were wound at 2000 fpm and a nip load of 8 lbf. The first set was unwound after 24 hours, the decrease in air volume was recorded and the average air layer thickness calculated. It was observed that the air layer thickness had diminished by about 10 μ inch on an average. The other set of rolls were unwound after three days and an additional decrease in air layer thickness by about 5 μ inch was observed.

Some interesting observations were made while unwinding these rolls, as compared to the rolls unwound immediately after winding. The rolls that were unwound soon after winding displayed typical characteristics as soon as they were placed in the bubblerimeter, viz., a lot of air bubbles could be seen surfacing the water in the bubblerimeter by the time the conical hood was hooked up for air collection, These bubbles came out at a fast rate, that impeded their estimation. The bubblerimeter has to be calibrated after the roll is placed inside it and the fastest this could be done was in a minute, but a lot of air was seen escaping during this time, which could not be accounted for since the rate of escape was unknown.

Further there is a spurt of air escape during the unwinding of the first few web layers, apparently there is a relatively larger amount of air in the outer layers but as the unwinding operation progresses the release of air bubbles becomes more consistent towards the inner layers. It would be safe to generalize that when unwinding a roll immediately after winding, ignoring the air escape from the first few layers of the web unwound, the amount of air collected as a function of time is nearly constant, indicating the consistency of the air layer thickness. Thus it can be assumed that the average air

layer thickness is the actual air layer thickness itself. The point to be emphasized here is that immediately after the winding operation the average air layer thickness would give a reasonable estimate of the absolute air layer thickness. The only shortcoming however is the failure of the existing apparatus to trap the air initially.

Fig.17 shows the rate of air escape in the bubblerimeter immediately after the winding operation. The volume of air collected is plotted as a function of the length of the roll at various times during the unwinding operation, for two different rolls 1500 ft. and 1500 mts. long respectively. Table IX in Appendix shows the recorded results.

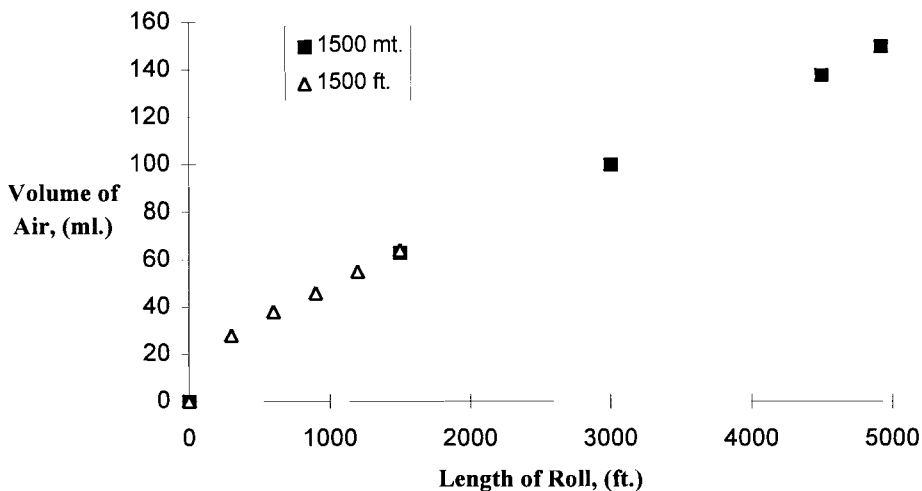


Figure 17. Volume of Air Collected at Various Lengths of the Unwinding Roll.

In contrast when unwinding a roll after sufficient lengths of time (e.g., 8, 16, 24 hours etc.) the observations made were quite different. As opposed to the fast escape of air bubbles observed in the previous case, very few bubbles could be seen escaping from

the roll edges and hence by the time the apparatus was ready to collect the air, hardly any bubbles surfaced and most of them were seen sticking to the roll edges, thus, in this case all the air collected was accounted for. Only when the roll started unwinding could one see the air bubbles rising up, even so at a slow rate. This rate kept decreasing as the roll unwound and there were times when no air bubbles could be seen for considerable lengths of the roll, and towards the end there was hardly any air collected in the apparatus.

A series of tests showed that, of all the air that was collected about 60% of it was collected during the unwinding of the first 400 ft. of the 1500 ft. long roll. This phenomenon questions the validity of using an average air layer thickness calculation for rolls kept for significant lengths of time (e.g., 8, 16, 24 hours etc.), because of the lot of air collected, which has been experimentally proven here to be present in the first few feet of the roll, is actually being split up over the entire length of the roll. It is for this reason that 1500 meters of roll unwound after 24 hours might have a smaller average air layer thickness than 1500 feet of it unwound after the same time. Moreover, the time taken to wind a roll 1500 meters long at 2000 fpm is about 2 min. and 30 secs., as opposed to the 53 secs needed to wind 1500 ft. of roll at the same speed. Thus in the former case while the roll builds up the air entrained in the lower layers has more time to escape and thus will escape unaccounted for. Added to this, the built-up of layers exerts additional pressure on the lower layers thereby squeezing out the entrained air more vigorously.

Fig.18 shows the volume of air collected in the bubblerimeter when the roll (1500 ft. long) was unwound after 3 days, as a function of the length of the unwinding roll.

Also it shows a comparison with similar data obtained for the roll that was immediately unwound. Due to the limited availability of the material a similar comparison for 1500 mts. of roll could not be made. Table X in Appendix shows the recorded results.

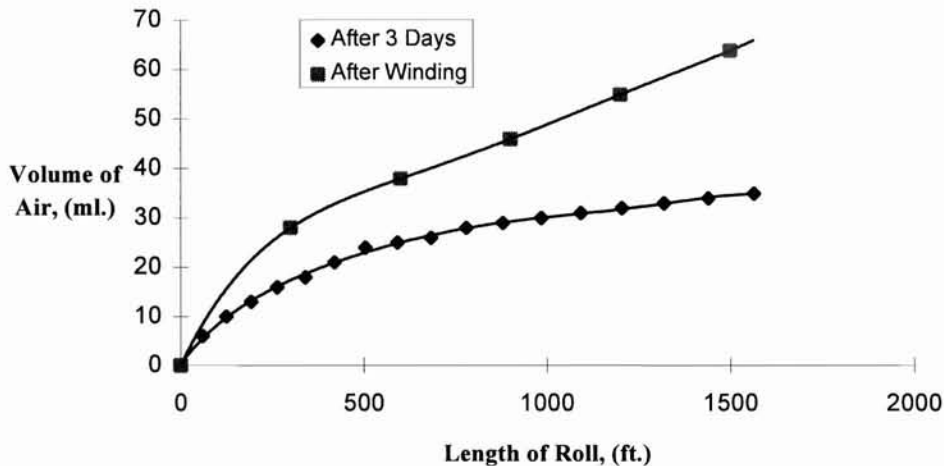


Figure 18. Comparison of the Volume of Air Collected Immediately and 3 Days After Winding, as the Roll Unwinds.

Since the amount of air collected after 24 hours showed a decrease in air layer thickness by 10μ inch it was expected that after three days the decrease would be even more, but it turned out to be 5μ inch, which implied that the rate of air escape had slowed down considerably. This led to reducing the time prior to unwinding and measuring the volume of air well before the 24 hour time period.

New rolls were wound and unwound again, after 8 and 16 hours respectively. Surprisingly they had roughly the same amount of air that was left in the roll after 24

hours. This meant that a lot of air that could have escaped had done so immediately after winding and the remaining was left to discharge at very slow rates, over periods of days. Also it has been mentioned before that rolls placed in the bubblerimeter immediately after winding had a tendency to release a lot of air bubbles at a fast rate. This reinforces the fact that a lot of the entrained air escapes during and immediately after winding. Thus the rate of air escape had to be studied shortly after winding.

A series of tests were performed and the air collected at intervals of 1, 3 and 10 minutes after the winding operation which took 53 seconds on an average. By the time the winding operation was terminated and the roll placed in the bubblerimeter ready to be unwound 1 minute and 53 seconds had elapsed. This time has been added to all time intervals after which the rolls have been unwound. Table XI in Appendix displays the data recorded for the above tests and Table XII compares the values derived theoretically from the squeeze film damper expression (Eq. (17), Chapter II) with the experimental values.

The data obtained from all these experiments was grouped systematically and analyzed using a spreadsheet program that displayed the rate of decrease of air layer thickness as a function of time as a 2 dimensional plot. The theoretical results from the squeeze film damping equation were also modeled similarly and formed a basis for comparison with the experimental results. Figures 19 & 20 show the rate of air escape as a function of time for the two sets of experiments and a comparison of theory and experiment respectively.

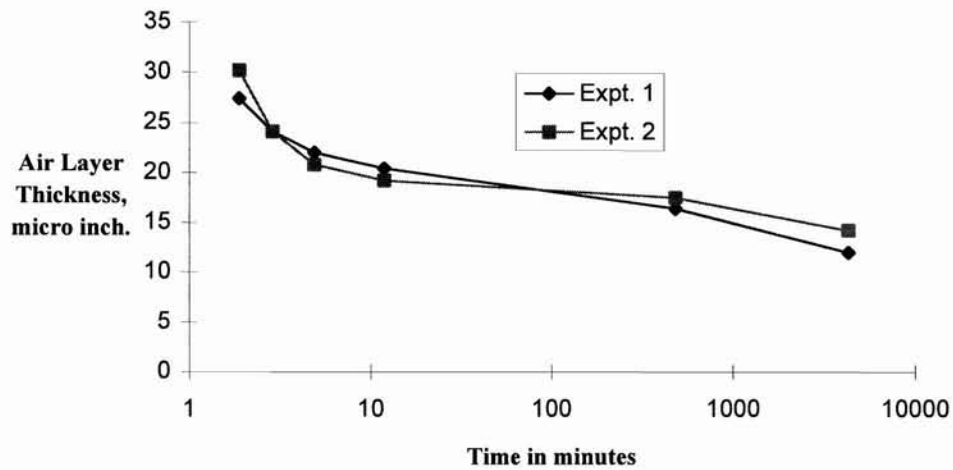


Figure 19. Air Escape as a Function of Time (Experimental Results).

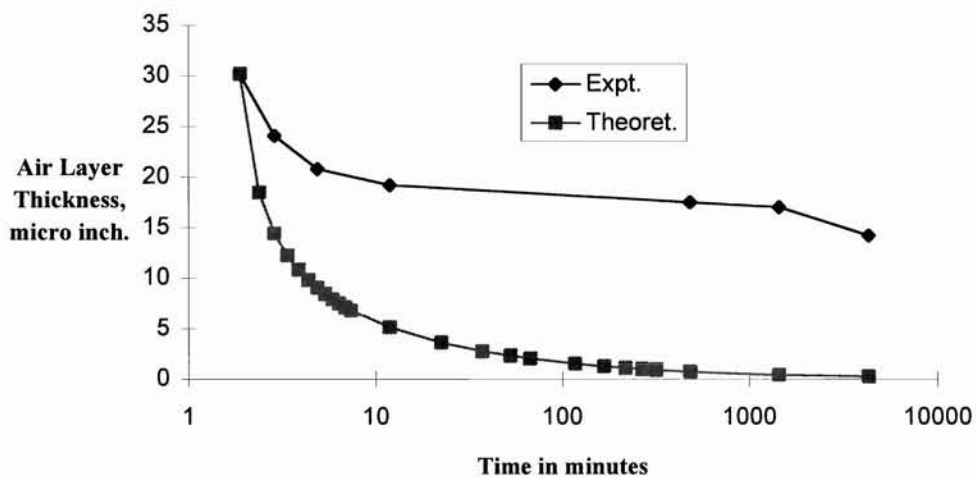


Figure 20. Air Escape as a Function of Time (Comparison Of Theory and Experiment).

Comparison of Theory and Experiment

As can be seen in Fig. 20 the theoretical results display a drastic decrease in air layer thickness during the first 5 to 10 minutes after winding the roll. The air layer drops from 30.2 μ inch at 1min and 53secs to about 5.1 μ inch at 11min and 53secs. On the contrary the experimental values of the air layer thickness decay from 30.2 μ inch to 19.2 μ inch over the same time range, thus displaying a less drastic air escape. In other words, 83% of the air entrapped when winding a roll at 2000 fpm and 8 lbf nip load escapes 10 minutes after the winding operation according to the squeeze film damper prediction, whereas the experiments show the escape to be 36%. Even though the amount of air escape predicted by the theory and experiment fall roughly about 50% apart a promising feature is the similarity in the rates, i.e., as a function of time the experimental plot behaves like the theoretical one. A large amount of air escapes during the first 10 minutes after winding and then we have a plateau for the next 16 to 24 hours, a further decrease is then observed only over periods of days (3 days in the experimental study). The theoretical plot also depicts a similar trend where most of the air escapes during the first 10 minutes after winding and then the rate becomes more or less a plateau for large time periods. Based on the above discussion and a comparison of theory and experiment it can be said that the entrained air is somehow being obstructed on its way out after the winding operation which may not be an ideal case as that assumed by the squeeze film damper equation.

The squeeze film damper equation assumes the two contacting surfaces to be perfect. On the contrary the contacting surfaces used in the experiments have some irregularities on a micro inch scale, which are bound to affect the average air layer thickness, which has the same orders of magnitude. Also it is a common observation that when a web is trimmed to its exact width the edges that are slit are slightly thicker than the web caliper depending on the type of slitting operation employed.

The presence of bumps at the roll edges could obstruct the air escape significantly. This has been illustrated by the drawing below, which exaggerates two web surfaces in contact. Further, as the roll builds up these bumps overlap and press relatively harder on each other than the rest of the overlapping layers in the roll. This could possibly magnify the phenomenon of obstruction of entrained air.

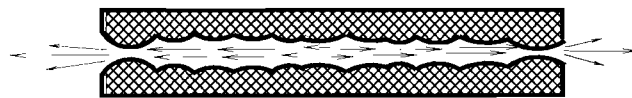


Figure 21. Bumps at the Roll Edges Obstructing the Escape of Entrained Air.

Another factor that could possibly affect the rate of air escape is the non-uniform pressure distribution along the width of the web. It has been proven in previous studies [3] that, under its own weight and the pressure force exerted by the two ends of the roll the film deforms as shown below:



Figure 22. Non-uniform Pressure Distribution Along the Web Width.

The above illustration explains for itself the bottlenecks created at the two extremities of the roll, which prevent the air from escaping. In fact the pressure profile of the pressure force exerted predicts a smaller value at the center of the roll and a little higher value towards the ends [3].

The two phenomenon explained above seem to have a combined effect on the rate of air escape. The bumps at the roll edges coupled with a higher pressure created there impede the air from escaping at a desired rate.

CHAPTER IX

SUMMARY AND CONCLUSIONS

This study has attempted to verify a winding model that would incorporate the entrained air, and a squeeze film damping equation to model the escape of air over time. It has also verified the decrease in radial modulus due to the presence of entrained air witnessed by Covell [5]. In other words, it has studied the factors which are known to contribute to a decrease in radial pressure during centerwinding with a force loaded nip roller.

Based on the experimental results obtained and comparing them with the results obtained from theoretical models the following conclusions can be derived:

- 1.) The air layer entrained during high speed winding with a nip roller is comparable to the theoretical minimum film thickness (h_0) derived by Chang (Eq.(41)). A more practical case would be Chang's h_c prediction (Eq.(42)) since it considers the expansion of the air film after it passes away from the nip, but the air loss from the roll edges is not considered in deriving h_c (or any other air film thickness derivations for that matter) hence it is possibly overestimating the results. Further, there is a possible transition from a hydrodynamic regime to elasto-hydrodynamic conditions towards high nip loads (e.g. 32, 48 lbf).

2.) Even small nip loads can affect the air layer thickness, so to get reasonable results it is necessary that the nip load be controlled precisely so as to minimize the fluctuations encountered during nip roll bounce. Moreover, the radial modulus of the nip, if it is a hollow cylindrical roller should be used instead of the elastic modulus for estimating the air layer thickness.

3.) The presence of entrained air reduces the radial modulus, E_r of the wound roll considerably by decreasing the radial pressure. Further, the radial modulus is a dynamic property of the roll which depends on radius of the roll and air film thickness.

4.) The bubblerimeter can be used as an air collection device as first documented by Covell [5], even though it may not be as sophisticated as laser reflectance probes, since it gives a simple and accurate account of air entrained for non-permeable (plastic) films.

5.) Most of the air that is entrained escapes during and immediately after winding.

6.) Finally, the air escaping from a wound roll can be modeled using a modified version of the squeeze film damping equation that would take into account the fluid dynamics in between the two web surfaces with irregularities towards the edges.

Future Work

The following section explores the various possibilities that could be investigated to obtain a much more sophisticated air entrainment model,

1.) It has been proven in this study that air is present immediately after winding, a technique to measure the air present in the first few seconds after winding if devised would give a clear understanding of the phenomenon at work during air discharge from the wound roll. The escape of air during the winding operation is another area that needs to be closely monitored and estimated for including the fluid dynamics aspect, which plays a significant role in air entrainment experiments coupled with the solid mechanics aspect.

2.) A procedure needs to be formulated for proper determination of E_b 's and E_r 's since the air film thickness h_0 and E_r are inter-related, and E_b in turn is related to E_r .

3.) Applying the equivalent radial modulus to study the air layer, when its value falls between the mean surface roughness and the maximum asperity height of the film.

4.) Measuring the air layer thickness as a function of the roll radius would contribute to modifying the existing models which assume an average air layer thickness throughout the wound roll.

5.) Lastly, the effect of nip roll dynamics on entrained air could also be included in the winding model.

REFERENCES

1. Bertram, N. and Eshel, A. "Recording Media Archival Attributes." RADC-TR-80-123, pp. 68-73, April 1980.
2. Blevins, Applied Fluid Dynamics Handbook. pp.503.
3. Bouquerel, F. "Theoretical and Experimental Study of Winding of Thin Plastic Films: Aerodynamics Effects." Ph.D Thesis, Central University of Lyon, France.
4. Chang, Y.B. "Air Entrainment With a Force Loaded Nip Roller." Technical Review and Industry Advisory Board Meeting, WHRC., May 1994.
5. Covell, K. Scott "The Effect of a Nip Roller on Entrained Air During High Speed Winding.", Master's Thesis, Department of Mechanical and Aerospace Engineering, Oklahoma State University, 1994.
6. Good, J.K. and Holmberg, M.W. "The Effect of Air Enrainment in Centerwound Rolls." Proceedings of the Second International Web Handling Conference, April 1993.
7. Good, J.K. Wu, Z. and Fikes, M.W.R. "The Internal Stresses in Wound Rolls With the Presence of a Nip Roller." accepted for publication in the ASME Journal of Applied Mechanics, 1992.
8. Hakiel, Z. "Nonlinear model for Wound Roll Stresses." TAPPI Journal, Volume 70, No. 5, pp. 113-117, 1987.
9. Hamrock, B.J. and Dowson, D. Ball Bearing Lubrication. John Wiley & Sons, pp. 188-89 and 280-82, 1981.
10. Holmberg, M.W. "Theoretical and Experimental Studies of Air Entrainment in Wound Rolls." Master's Thesis, Department of Mechanical and Aerospace Engineering, Oklahoma State University, 1992.
11. Knox, K.L. and Sweeny, "Fluid Effects Associated with Web Handling." Ind. Engr. Chem. Proc., vol. 10, pp. 201-205, October 1971.
12. Xu, Y. "Computing Stress Distributions in Centerwound Rolls from Web Surface Charecteristics." Ph.D. Thesis, Department of Mechanical and Aerospace Engineering, Oklahoma State University, 1992.

APPENDIX

TABLE I

VOLUME OF AIR COLLECTED FOR TWENTY FOUR INDIVIDUAL WINDING EXPERIMENTS

Nip Load lbf	Speed fpm	Vol. of Air (uncorrected) ml.	Vol. of Air (corrected) ml.	Air Layer Thickness micro in.
4	500	44	32.98	18.6
8		35	24.25	13.7
12		27	16.49	9.3
16		23	12.61	7.1
32		20	9.7	5.4
48		20	9.7	5.4
4	1000	57	45.59	25.7
8		54	42.68	24.1
12		49	37.83	21.3
16		46	34.92	19.7
32		38	27.16	15.3
48		33	22.31	12.6
4	1500	65	53.35	30.1
8		63	51.41	29.0
12		57	45.59	25.7
16		57	45.59	25.7
32		46	34.92	19.7
48		45	33.95	19.1
4	2000	80	67.9	38.3
8		67	55.29	31.2
12		61	49.47	27.9
16		56	44.62	25.2
32		50	38.8	21.9
48		40	29.1	16.4

TABLE II

COMPARISON OF THEORETICAL VALUES FROM BERTRAM AND ESHEL'S
HYDRODYNAMIC EQUATION WITH THE EXPERIMENTAL RESULTS

Nip Load lbf	Speed fpm	Theoretical Air Layer Thickness (h_0) micro in.	Experimental Air Layer Thickness micro in.	Deviation micro in.
4	500	1.8	18.6	-16.8
8		0.9	13.7	-12.8
12		0.6	9.3	-8.7
16		0.5	7.1	-6.6
32		0.3	5.4	-5.1
48		0.2	5.4	-5.2
4	1000	3.5	25.7	-22.2
8		1.8	24.1	-22.3
12		1.2	21.3	-20.1
16		0.9	19.7	-18.8
32		0.5	15.3	-14.8
48		0.3	12.6	-12.3
4	1500	5.2	30.1	-24.9
8		2.6	29.0	-26.4
12		1.8	25.7	-23.9
16		1.3	25.7	-24.4
32		0.7	19.7	-19.0
48		0.5	19.1	-18.6
4	2000	6.9	38.3	-31.4
8		3.5	31.2	-27.7
12		2.3	27.9	-25.6
16		1.8	25.2	-23.4
32		0.9	21.9	-21.0
48		0.6	16.4	-15.8

Bertram and Eshel's hydrodynamic equation given below was used to derive the theoretical values tabulated on the previous page, the following section specifies the values that were varied and those which were held constant to obtain the film thickness.

$$L = \frac{4\mu UR_e}{h_0} + \frac{4T\sqrt{2R_e h_0}}{3\pi R_0}$$

L = Nip Load, varied as 4,8,12,16,32 and 48 lbf. for each winding velocity used.

U = Winding Velocity, varied as 500,1000,1500 and 2000 fpm.

T = Web Line Tension, held constant at 0.48 lbf/in. throughout experimentation.

R_e = Equivalent Radius, calculated as 1.085 inch.

μ = Dynamic Viscosity of Air 2.6E-9 lbf-sec/in.²

R₀ = Radius of Wound Roll, measured as 2.4 inch. an average

π = 3.1414.

h₀ = Air Film Thickness, from 24 different combinations of velocities and nip loads

TABLE III

COMPARISON OF THEORETICAL VALUES FROM HAMROCK AND DOWSON'S ELASTO-HYDRODYNAMIC MINIMUM AIR FILM THICKNESS EQUATION WITH THE EXPERIMENTAL RESULTS

Nip Load lbf	Speed fpm	Theoretical Air Layer Thickness (h_0) micro in.	Experimental Air Layer Thickness micro in.	Deviation micro in.
4	500	11.1	18.6	-7.5
8		9.8	13.7	-3.9
12		9.1	9.3	-0.2
16		8.6	7.1	1.5
32		7.5	5.4	2.1
48		6.9	5.4	1.5
4	1000	17.4	25.7	-8.3
8		15.4	24.1	-8.7
12		14.2	21.3	-7.1
16		13.4	19.7	-6.3
32		11.7	15.3	-3.6
48		10.8	12.6	-1.8
4	1500	22.6	30.1	-7.5
8		20.0	29.0	-9.0
12		18.5	25.7	-7.2
16		17.5	25.7	-8.2
32		15.2	19.7	-4.5
48		14.0	19.1	-5.1
4	2000	27.3	38.3	-11.0
8		24.2	31.2	-7.0
12		22.3	27.9	-5.6
16		21.1	25.2	-4.1
32		18.4	21.9	-3.5
48		16.9	16.4	0.5

Hamrock and Dowson's elasto-hydrodynamic equation given below was used to derive the theoretical values tabulated on the previous page, the following section specifies the values that were varied and those which were held constant to obtain the film thickness.

$$h_0 = R_x 7.43U^{0.65}W^{-0.21}$$

where,

$$U = \frac{\mu u}{E' R_x} \quad \text{where} \quad u = \frac{u_a + u_b}{2}, \quad \text{and} \quad W = \frac{F}{E' R_x^2} \quad \text{where} \quad R_x = \frac{1}{\frac{1}{R_n} + \frac{1}{R_r}}$$

F = Normal Applied Load, lbf (including tension component $T \sin 45$), (e.g., 4lb nip load plus $2.88 \sin 45$ etc.)

u = Average of Nip and Roll Velocities, varied as 500,1000,1500 and 2000 fpm.

T = Winding Tension, held constant at 2.88 lbf throughout experimentation.

R_x = Equivalent Radius, calculated as 1.085 inch.

R_n = Radius of Nip, 2 in.

R_r = Radius of Roll, 2.4 in.

E' = Calculated Effective Modulus, psi.

E_a = Modulus of Nip, 675 psi.

E_b = Modulus of Roll, (determined by Covell[5] using contact tests) 8200,12800,19800, 27600,37000 and 47000 psi corresponding to 4,8,12,16,32 and 48 lbf nip loads.

μ = Dynamic Viscosity of Air $2.6E-9$ lbf-sec/in.²

h_0 = Air Film Thickness, from 24 different combinations of velocities and nip loads

TABLE IV

COMPARISON OF THEORETICAL VALUES CALCULATED FROM CHANG'S ELASTO-HYDRODYNAMIC EQUATION FOR COMPRESSED AIR FILM WITH THE EXPERIMENTAL RESULTS

Nip Load lbf	Speed fpm	Theoretical Air Layer Thickness (h_0) micro in.	Experimental Air Layer Thickness micro in.	Deviation micro in.
4	500	17.1	18.6	-1.5
8		11.9	13.7	-1.8
12		9.6	9.3	0.3
16		8.3	7.1	1.2
32		5.8	5.4	0.4
48		4.8	5.4	-0.6
4	1000	28.1	25.7	2.4
8		19.6	24.1	-4.5
12		15.8	21.3	-5.5
16		13.6	19.7	-6.1
32		9.6	15.3	-5.7
48		7.8	12.6	-4.8
4	1500	37.7	30.1	7.6
8		26.2	29.0	-2.8
12		21.2	25.7	-4.5
16		18.3	25.7	-7.4
32		12.9	19.7	-6.8
48		10.5	19.1	-8.6
4	2000	46.3	38.3	8.0
8		32.3	31.2	1.1
12		26.1	27.9	-1.8
16		22.5	25.2	-2.7
32		15.8	21.9	-6.1
48		12.9	16.4	-3.5

Chang's elasto-hydrodynamic equation given below was used to derive the theoretical values tabulated on the previous page, the following section specifies the values that were varied and those which were held constant to obtain the film thickness.

$$h_0 = R_x 8.5U^{0.72}W^{-0.5}G^{-0.48}$$

where,

$$U = \frac{\mu u}{P_a R_x}, \quad W = \frac{F}{P_a R_x}, \quad \text{and} \quad G = \frac{E}{P_a} \quad \text{where} \quad E = \frac{1}{\frac{1 - \nu_a^2}{E_a} + \frac{1 - \nu_b^2}{E_b}}$$

F = Nip Loading per Unit Width of roller, pli (e.g., 4/6,8/6,12/6 pli etc.)

u = Average of Nip and Roll Velocities, varied as 500,1000,1500 and 2000 fpm.

T = Winding Tension, held constant at 0.48 lb/in. throughout experimentation.

P_a = Ambient Pressure, 14.7 psi.

R_x = Equivalent Radius, calculated as 1.085 inch.

E = Calculated Effective Modulus, psi.

E_a = Modulus of Nip, 675 psi.

E_b = Modulus of Roll, (determined by Covell[5] using contact tests) 8200,12800,19800, 27600,37000 and 47000 psi corresponding to 4,8,12,16,32 and 48 lbf nip loads.

μ = Dynamic Viscosity of Air 2.6E-9 lbf-sec/in.²

h₀ = Air Film Thickness, from 24 different combinations of velocities and nip loads

TABLE V

COMPARISON OF THEORETICAL VALUES CALCULATED FROM CHANG'S HYDRODYNAMIC EQUATION FOR DECOMPRESSED AIR FILM WITH THE EXPERIMENTAL RESULTS

Nip Load lbf	Speed fpm	Theoretical Air Layer Thickness (h_c) micro in.	Experimental Air Layer Thickness micro in.	Absolute Error micro in.
4	500	2.3	18.6	-16.3
8		1.1	13.7	-12.6
12		0.8	9.3	-8.5
16		0.6	7.1	-6.5
32		0.3	5.4	-5.1
48		0.2	5.4	-5.2
4	1000	4.5	25.7	-21.2
8		2.3	24.1	-21.8
12		1.5	21.3	-19.8
16		1.1	19.7	-18.6
32		0.6	15.3	-14.7
48		0.4	12.6	-12.2
4	1500	6.8	30.1	-23.3
8		3.4	29.0	-25.6
12		2.3	25.7	-23.4
16		1.7	25.7	-24.0
32		0.8	19.7	-18.9
48		0.6	19.1	-18.5
4	2000	9.0	38.3	-29.3
8		4.5	31.2	-26.7
12		3.0	27.9	-24.9
16		2.3	25.2	-22.9
32		1.1	21.9	-20.8
48		0.8	16.4	-15.6

Chang's hydrodynamic equation given below was used to derive the theoretical values tabulated on the previous page, the following section specifies the values that were varied and those which were held constant to obtain the film thickness.

$$h_c = \frac{16 \mu U R_e}{3 L}$$

L = Nip Load, varied as 4,8,12,16,32 and 48 lbf. for each winding velocity used.

U = Winding Velocity, varied as 500,1000,1500 and 2000 fpm.

R_e = Equivalent Radius, calculated as 1.085 inch.

μ = Dynamic Viscosity of Air 2.6E-9 lbf-sec/in.²

π = 3.1414.

h_c = Decompressed Air Film Thickness, from 24 different combinations of velocities and nip loads

TABLE VI

COMPARISON OF THEORETICAL VALUES CALCULATED FROM CHANG'S ELASTO-HYDRODYNAMIC EQUATION FOR DECOMPRESSED AIR FILM WITH THE EXPERIMENTAL RESULTS

Nip Load lbf	Speed fpm	Theoretical Air Layer Thickness (h_c) micro in.	Experimental Air Layer Thickness micro in.	Absolute Error micro in.	h_c/h_0
4	500	30.8	18.6	12.2	1.8
8		26.6	13.7	12.9	2.2
12		24.4	9.3	15.1	2.5
16		23.0	7.1	15.9	2.8
32		20.0	5.4	14.6	3.4
48		18.4	5.4	13.0	3.9
4	1000	50.4	25.7	24.7	1.8
8		43.5	24.1	19.4	2.2
12		39.9	21.3	18.6	2.5
16		37.6	19.7	17.9	2.8
32		32.7	15.3	17.4	3.4
48		30.1	12.6	17.5	3.9
4	1500	67.2	30.1	37.1	1.8
8		58.0	29.0	29.0	2.2
12		53.3	25.7	27.6	2.5
16		50.2	25.7	24.5	2.8
32		43.6	19.7	23.9	3.4
48		40.2	19.1	21.1	3.8
4	2000	82.4	38.3	44.1	1.8
8		71.2	31.2	40.0	2.2
12		65.3	27.9	37.4	2.5
16		61.5	25.2	36.3	2.7
32		53.5	21.9	31.6	3.4
48		49.3	16.4	32.9	3.8

Chang's elasto-hydrodynamic equation given below was used to derive the theoretical values tabulated on the previous page, the following section specifies the values that were varied and those which were held constant to obtain the film thickness.

$$h_c = R_x 12.5U^{0.71}W^{-0.2}G^{-0.23}$$

where,

$$U = \frac{\mu u}{P_a R_x}, \quad W = \frac{F}{P_a R_x}, \quad \text{and} \quad G = \frac{E}{P_a} \quad \text{where} \quad E = \frac{1}{\frac{1 - \nu_a^2}{E_a} + \frac{1 - \nu_b^2}{E_b}}$$

F = Nip Loading per Unit Width of roller, pli (e.g., 4/6,8/6,12/6 pli etc.)

u = Average of Nip and Roll Velocities, varied as 500,1000,1500 and 2000 fpm.

T = Winding Tension, held constant at 0.48 lb/in. throughout experimentation.

P_a = Ambient Pressure, 14.7 psi.

R_x = Equivalent Radius, calculated as 1.085 inch.

E = Calculated Effective Modulus, psi.

E_a = Modulus of Nip, 675 psi.

E_b = Modulus of Roll, (determined by Covell[5] using contact tests) 8200,12800,19800, 27600,37000 and 47000 psi corresponding to 4,8,12,16,32 and 48 lbf nip loads.

μ = Dynamic Viscosity of Air 2.6E-9 lbf-sec/in.²

h_c = Decompressed Air Film Thickness, from 24 different combinations of velocities and nip loads

TABLE VII

COMPARISON OF EXPERIMENTAL RESULTS OBTAINED FOR THE RUBBER NIP
AND THE HOLLOW ALUMINUM NIP

Speed	Nip Load	Air collected after one minute after winding* winding time : For 1500 ft. = 53 Secs., For 1500mts. = 2Min&30 Secs.							
		Rubber Nip				Hollow Aluminum Nip			
fpm	lbf	1500 mts.		1500 ft.		1500 mts.		1500 ft.	
		ml.	μ inch	ml.	μ inch	ml.	μ inch	ml.	μ inch
2000	8	135.8	23.4	55.3	31.2	128	22.1	52.3	29.6
2000	8	125.1	21.6	59.2	33.4	-	-	-	-

* All data taken for two different rolls one 1500 mts. and the other 1500 ft. long.

TABLE VIII
 RADIAL PRESSURES AS A FUNCTION OF NORMALIZED RADIUS

R/Rc	P (using Er stack) psi.	P (using Er eq) psi.	P (using Er air) psi.
1	184.1033	111.8518	5.459071
1.032021	154.7302	88.54622	3.216585
1.064448	134.5964	74.32354	3.198831
1.096875	119.5859	67.88147	3.182084
1.129301	107.4788	63.32581	3.166257
1.161728	96.93085	59.50649	3.151277
1.194155*	85.04928	55.73399	3.137076
1.226581	77.19245	51.52646	3.123595
1.259008	66.85479	46.47226	3.11078
1.291435	55.5874	40.1336	3.098582
1.323861	42.92696	31.94269	3.086956
1.356288	28.29851	21.01056	3.07548
1.388715	10.78037	9.783308	2.93404

* Normalized radius corresponding to the mid-point of the wound roll.

TABLE IX

VOLUME OF AIR COLLECTED IMMEDIATELY AFTER WINDING AS A
FUNCTION OF THE LENGTH OF THE ROLL UNWOUND*

Speed fpm	Nip Load lbf	1500mts.		1500ft.	
		Length ft.	Vol. of Air ml.	length ft.	Vol. of Air ml.
2000	8	1500	63	300	28
		3000	100	600	38
		4500	138	900	46
		4920	150	1200	55
				1500	64

* Data taken for two different rolls 1500 mts. and 1500 ft. long respectively.

TABLE X

COMPARISON OF THE AIR COLLECTED FROM TWO ROLLS UNWOUND 3 DAYS AFTER AND IMMEDIATELY AFTER WINDING RESPECTIVELY, AS A FUNCTION OF THEIR LENGTHS

Speed fpm	Nip Load lbf	3 Days After Winding		Immediately After Winding	
		Length ft.	Vol. of Air ml.	Length ft.	Vol. of Air ml.
2000	8	60	6	-	-
		124	10	-	-
		192	13	-	-
		264	16	-	-
		300	-	300	28
		340	18	-	-
		420	21	-	-
		504	24	-	-
		592	25	-	-
		600	-	600	38
		684	26	-	-
		780	28	-	-
		880	29	-	-
		900	-	900	46
		984	30	-	-
		1092	31	-	-
		1200	-	1200	55
		1204	32	-	-
1320	33	-	-		
1440	34	-	-		
1500	-	1500	64		

TABLE XI

AIR LAYER THICKNESS AS A FUNCTION OF TIME FOR THREE SETS OF ROLL SAMPLES

Air Layer Thickness micro in.	Time [†]							
	(in minutes)				(in hours)			
	X*	X*+1	X*+3	X*+10	8	16	24	3X24
Sample Roll Number								
1	29	25.2	22	17.5	20.8	17.5	16.4	14.2
2	27.4	24.1	22	21.4	16.4	20.8	19.2	12
3	30.2	24.1	20.8	19.2	17.5	17.5	17	14.2

[†] Data taken for 1500 ft. of web wound at 2000 fpm and 8 lbf nip load.

* X represents 1 min & 53 seconds (the time taken to set up the air collection apparatus).

TABLE XII

COMPARISON OF THEORETICAL VALUES CALCULATED FROM SQUEEZE
FILM DAMPER EQUATION WITH EXPERIMENTAL RESULTS

Speed fpm	Nip Load lbf	Time minutes	Air Layer Thickness micro in.		
			Theoretical	Experimental	Deviation
2000	8	1.9	30.2	30.2	0.0
		2.9	14.4	24.1	-9.7
		4.9	9.1	20.8	-11.7
		11.9	5.1	19.2	-14.1
		481.9	0.7	17.5	-16.8
		1441.9	0.4	17	-16.6
		4321.9	0.2	14.2	-14.0

The squeeze film damper equation given below was used to obtain the theoretical decrease in the air film thickness as a function of time as tabulated on the previous page

$$t = \frac{\mu b L^3}{2W} \left[\frac{1}{h_2^2} - \frac{1}{h_1^2} \right]$$

μ = Viscosity of Air, 2.6E-9 lbf-sec/in².

$P = W/bL = 3$ psi. (calculated by Winder v4.0)

$L =$ Width of Web = 6 in.

$h_1 =$ Initial Air Film Thickness, 30.2 micro in. (assumed from experiment)

$t =$ Time Period for Decrease of h_1 to the Next Lower Value, 1,3,10 minutes etc.(from experiment).

$h_2 =$ Theoretically Calculated Corresponding to the Time Periods Used for Experiment (1,3,10 minutes etc),micro in.

TABLE XIII

COMPARISON OF THE RANGE OF DIMENSIONLESS PARAMETERS USED BY HAMROCK & DOWSON WITH THOSE ASSOCIATED WITH THE EXPERIMENTS

Hamrock & Dowson's Dimensionless Parameters		Experimental Dimensionless Parameters		Absolute Difference	
W	U	W	U	W	U
2.20E-04	5.14E-09	8.93E-03	4.07E-04	-8.71E-03	-4.07E-04
↓	↓	↓	↓	↓	↓
2.20E-03	5.14E-08	2.60E-02	1.67E-05	-2.38E-02	-1.66E-05

TABLE XIV

COMPARISON OF THE RANGE OF DIMENSIONLESS PARAMETERS USED BY
CHANG WITH THOSE ASSOCIATED WITH THE EXPERIMENTS

Chang's Dimensionless Parameters			Experimental Dimensionless Parameters		
W	U	G	W	U	G
6.27E-3	1.304E-8	6.8	0.0631	1.63E-8	49.8
↓	↓	↓	↓	↓	↓
0.3135	1.63E-7	340.1	0.523	6.52E-8	53.7

TABLE XV

INDIVIDUAL EFFECT OF WOUND ROLL MODULUS E_b AND NIP MODULUS E_a ON THE AIR LAYER THICKNESS (h_0) DERIVED BY HAMROCK AND DOWSON AND BY CHANG FOR THEIR ELASTO-HYDRODYNAMIC EQUATIONS

Modulus of Roll E_b /Nip E_a psi	h_0 for Ham&Dow., E_a held const. micro inch	h_0 for Chang, E_a held const. micro inch	h_0 for Ham&Dow., E_b held const. micro inch	h_0 for Chang, E_b held const. micro inch
100	61.94	90.11	54.71	78.69
500	35.85	49.62	27.38	36.98
1000	30.48	41.58	20.57	27.07
1500	28.40	38.49	17.53	22.74
2000	27.28	36.84	15.72	20.19
2500	26.59	35.81	14.49	18.47
3000	26.11	35.11	13.59	17.23
3500	25.76	34.60	12.90	16.28
4000	25.49	34.21	12.35	15.52
4500	25.28	33.90	11.90	14.91
5000	25.11	33.65	11.53	14.39
5500	24.97	33.45	11.21	13.96
6000	24.85	33.28	10.93	13.58
6500	24.75	33.13	10.69	13.25
7000	24.67	33.01	10.48	12.97
7500	24.59	32.90	10.29	12.71
8000	24.53	32.80	10.12	12.49
8500	24.47	32.72	9.97	12.28
9000	24.42	32.64	9.83	12.10
9500	24.37	32.57	9.71	11.93
10000	24.33	32.51	9.59	11.78
10500	24.29	32.46		
11000	24.26	32.41		
11500	24.23	32.36		
12000	24.20	32.32		
12500	24.17	32.28		
12800	24.16	32.26		

VITA

Humair A. Mohammed

Candidate for the Degree of

Master of Science

Thesis: RATE OF AIR ESCAPE FROM ROLLS WOUND AT HIGH SPEEDS
WITH A FORCE LOADED NIP

Major Field: Mechanical Engineering

Biographical:

Personal Data: Born in Hyderabad, India, April 20, 1970, the son Mohammed Manzoor Ahmed and Naima Azmath.

Education: Graduated from Little Flower High School, Hyderabad, India in June 1985; received Bachelor of Science degree in Mechanical Engineering from Osmania University, Hyderabad, India in June 1992; completed requirements for the Master of Science degree at Oklahoma State University, Stillwater, Oklahoma in May 1995.

Professional Experience: Research Assistant, Department of Mechanical and Aerospace Engineering, Oklahoma State University, January, 1994 to March, 1995; Teaching Assistant, August 1993 to December 1993.